Summer 8-2015

Spontaneous Firing of Sensory Neurons Modulates the Gain in the Downstream Circuit of a Simple Olfactory System

Matthew O'Neill
Washington University in St Louis

WASHINGTON UNIVERSITY IN ST. LOUIS

School of Engineering and Applied Science

Department of Biomedical Engineering

Thesis Examination Committee:
Baranidharan Raman, Chair
Dennis Barbour
Dan Moran

Spontaneous Firing of Sensory Neurons Modulates the Gain in the Downstream Circuit of a Simple Olfactory System

By

Matthew O'Neill

A thesis presented to the School of Engineering
of Washington University in St. Louis in partial fulfillment of the
requirements for the degree of
Master of Science

August 2015

Saint Louis, Missouri

Contents

List of Figures

List of Tables

Acknowledgements

I would like to thank my research advisor, Dr. Raman, and the members of his lab for their continual support throughout this project. Nalin Katta, Debajit Saha, and Chao Li were especially invaluable resources for ideas and resolutions. I would also like to send appreciation to the members of my committee for taking the time to read this thesis, attend my defense, and give valuable advice along the way. Additionally, I give special thanks to the Children's Discovery Institute, which provided the grant that not only allowed me to obtain the materials I needed for the project, but also provided some of the money that kept me afloat throughout my graduate school career. Finally, I would like to give the biggest thanks of all to my parents, Tom and Tracey, my sister, Sarah, and my brother-in-law, Doug. I could not have done this without you all, and would not be where or who I am today without any of you.

ABSTRACT OF THE THESIS

Spontaneous Firing of Sensory Neurons Modulates the Gain in the Downstream Circuit of a Simple Olfactory System

by

Matthew O'Neill

Master of Science in Biomedical Engineering

Washington University in St. Louis, 2015

Research Advisor: Professor Baranidharan Raman

In locusts and other insects, odorants are transduced into electrical signal by the olfactory receptor neurons and transmitted to central circuits for further processing. Previous studies have shown that exogenous variables (e.g., flow rates, humidity, temperature, odor mixtures, etc.) can influence the responses of the sensory neurons and therefore modulate the central circuits. However, how the sensory neuron activity is manipulated to achieve adaptive gain control in the following circuit is yet to be understood. It is possible that the magnitude of the stimulus-evoked response in the receptor neurons, their spontaneous activity, or both of these factors can change how information about a chemical cue is processed downstream. To this end, I studied the effects of modulating two different factors on the olfactory system (flow rate and relative humidity) at four levels of the olfactory system: individual olfactory receptor neurons (first-order neurons), the whole antenna (electroantennogram recordings), individual projection neurons in the antennal lobe of the brain (second-order neurons), and population antennal lobe activity as assayed by local field potential recordings in the mushroom body. We found that flow rate changes altered the magnitude of the stimulus-evoked responses in the antenna without altering the spontaneous activity levels. Whereas, changes in the relative humidity elicited a decrease in both response magnitude and baseline activity. Intriguingly, only the humidity modulation experiments brought about significant compensatory change in the spontaneous and odor-evoked activity of the second-order neurons in the antennal lobe. Therefore, our data and analysis

suggest that baseline activity of receptor neurons seems to play a key role in adapting the gain of the locust brain's central circuit.

Chapter 1 Introduction

Any animal's sense of smell is among its principle means of survival. Be it finding food, sensing predators, or finding a mate, olfaction is deeply engrained in the animal's ability to survive and thrive. It has been shown that there are remarkable similarities in the olfactory pathway over a wide range of animals [1]–[4]. In fact, the olfactory centers in the insect brain (the antennal lobe and mushroom body) have analogous structures in the human brain (the olfactory bulb and olfactory cortex, respectively) [1], [4]–[6]. The locust is certainly no different, and fully characterizing locust olfactory system may help understanding how chemical sensing systems in other animals works. While the central processing of olfactory signals in the brain is critical to the overall system, the activity and influence of the lower-order neurons must also be addressed.

The locust first senses an odor using olfactory receptor neurons (ORNs) in its antenna. The ORNs, or "first-order" neurons, each have their own baseline spontaneous firing rate (a DC signal) which may increase or decrease in response to odor stimulation, thus acting as the first level of odor sensing [7], [8]. It has also been suggested that ORN firing patterns contain information pertaining to odor identification [9]–[11]. When recording from ORNs extracellularly, as in this paper (see Methods), it is possible to obtain voltage spikes (i.e., action potentials) from individual cells. The spikes of each cell are recorded and separated to obtain the most accurate representation of each cell's behavior. These spikes can be reported either as raster plots-which denote the occurrence of a spike-or as summed as a peristimulus time histogram (PSTH). An example of both the raster and PSTH plots can be found in Figure 1.1. The strong change in spike frequency as shown in the raster plots and deflection in the PSTH plot immediately following odor onset makes it clear that the cell is responding to the stimulus.

Voltages measured in the whole antenna can be attributed to the net activity of the population of all ORNs. The whole antenna response is recorded by reading the voltage passing through the antenna via an electroantennogram (EAG). As the net spiking rate of the entire receptor neuron population increases in response to an odor stimulus, it causes a voltage deflection in the EAG, as shown in Figure 1.2. The magnitude of the voltage deflection is a reasonable measure of the strength of the antenna's response to the given odor stimulus. This is therefore indicative of the overall ORN activity in the antenna.

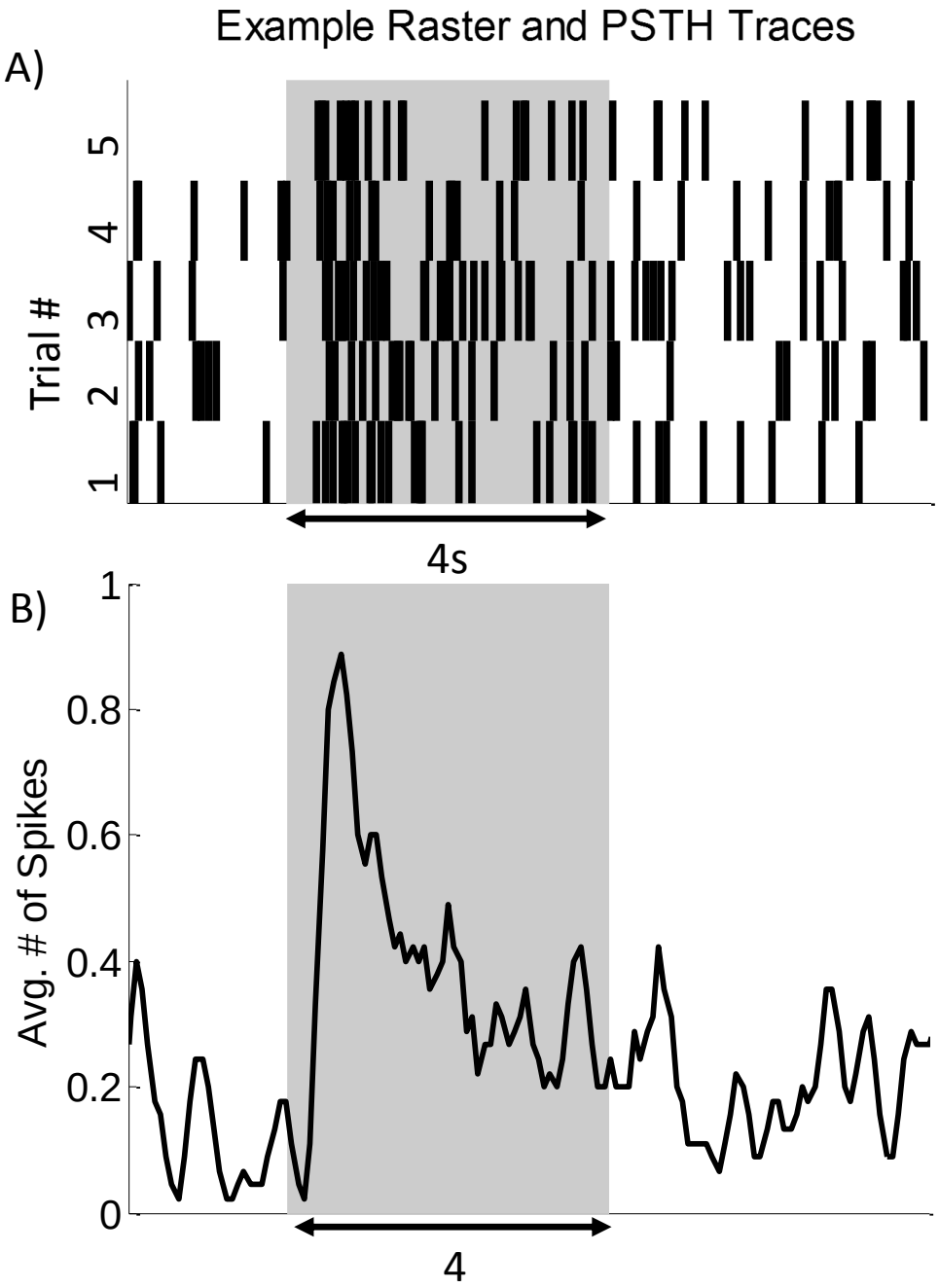

Figure 1.1: Representative raster plot and PSTH. A) A raster plot of a single cell. Bold lines represent a single action potential in the cell. Hexanol stimulation (as indicated by shaded rectangle) results in higher spiking activity. Spikes are summed in 75ms bins and averaged across trials to create the PSTH plot (B). Spiking activity returns to baseline after the odor offset. PN responses were analyzed in the same manner. Grey bar indicates the presence of the odor stimulus (1-octanol, here).

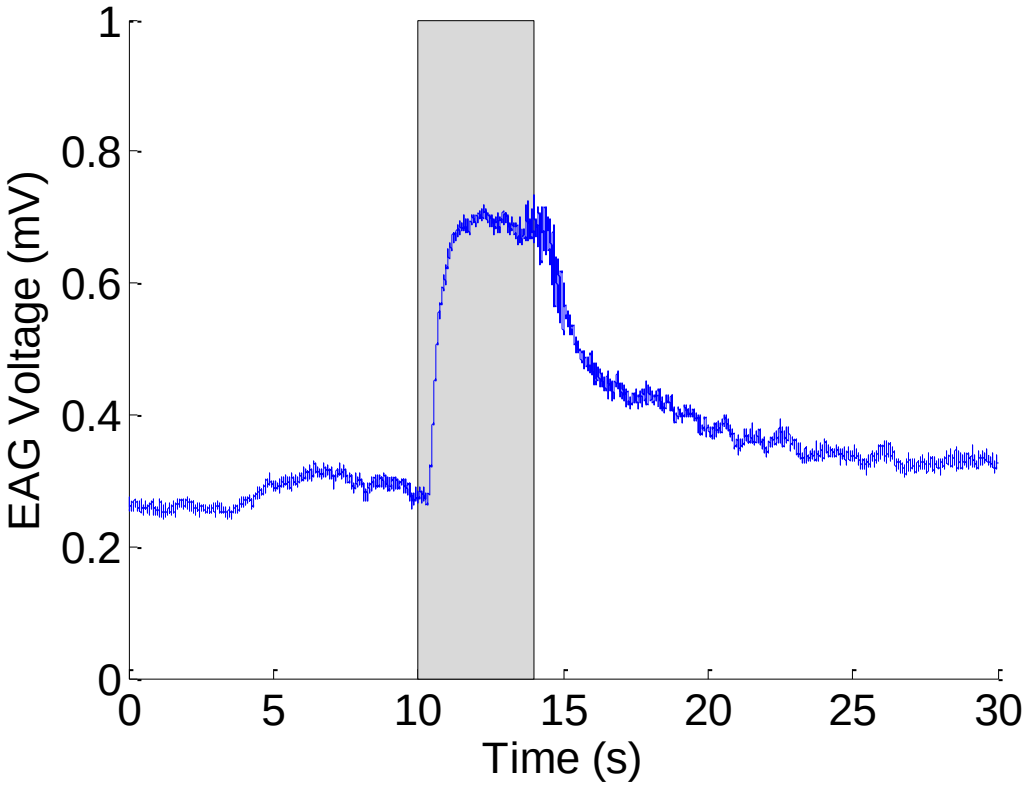

Figure 1.2: Representative electroantennogram plot. Electroantennograms measure the voltage across the whole antenna. This voltage exhibits an upward deflection in the presence of an odor stimulant (in this case, hexanol). The voltage slowly returns to baseline after the odor offset.

The activity of ORNs in the antenna are transmitted into the antennal lobe of the brain, where it is eventually received by projection neurons (PNs). PNs, like ORNs also have a specific response pattern to a given stimulus. It has been shown that their firing patterns have a critical role in odor identification [10], [12]. Projection neurons are frequently called second-order neurons [8]. Similar to the ORNs, in these experiments, a micropipette electrode makes extracellular recordings of the nearby neurons. As we are also looking at their spiking behavior, it follows that raster and PSTH plots are also valuable ways of observing their response. Again, we can see that the cell is responding to the odor stimulus due to the strong increase in firing rate soon after odor onset. It should be noted that some of the PNs demonstrated a response to the odor offset instead of-or, in some cases, in addition to-the onset response.

From the PNs in the antennal lobe, the signal is projected to Kenyon cells in the mushroom body, an area of the brain that has long been identified as a center of odor learning and memory [13], [14]. In the mushroom body, local field potential recordings (LFPs) of Kenyon cell activity demonstrate oscillatory electrical signals. Reporting the behavior of the mushroom body is noticeably different from the other two cell recordings presented here. Here, instead of individual cell readings, the ensemble activity is recorded by local field potential. These voltage readings are exhibited as oscillations of a relatively constant magnitude and frequency (Figure 1.3A&B). Shortly after odor presentation, there is a change in the magnitude and frequency of these oscillations. Spectrogram analysis is one of the most reasonable ways to report this data. In this analysis, the overall wave is broken into a combination of sine waves. Each of these waves has its own frequency and magnitude. In a spectrogram plot (Figure 1.3C), each frequency is analyzed over time. In each time bin, a frequency is assigned a power that corresponds to the magnitude of that frequency in the overall wave at the given time. After odor stimulation, one frequency tends to dominate others, as demonstrated by its much higher power. This response tends to dissipate relatively quickly over the odor pulse. Because the LFP measures oscillatory signal that originates in the antennal lobe, it allows us to examine the synchronicity of the neuron response [15]–[17]. We can evaluate changes in this synchronicity, be looking at the power of the dominant frequency. If this power is reduced, it suggests that synchronicity has been disrupted, indicating that changes have been made to the neurons' reaction time constants.

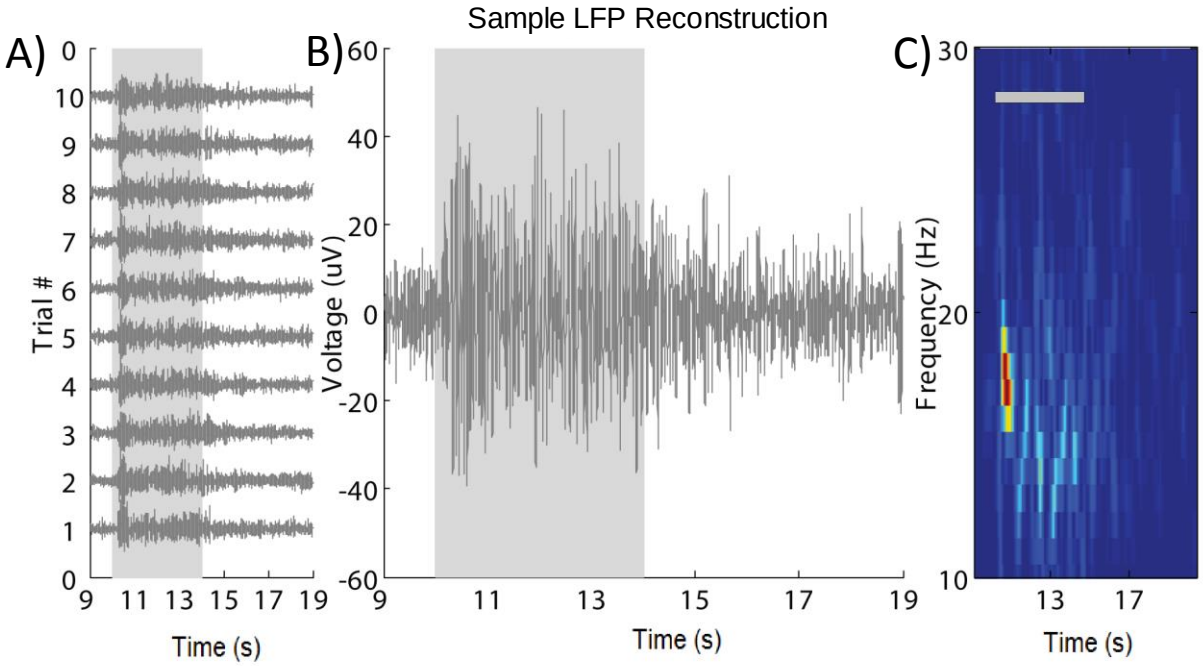

Figure 1.3: Representative mushroom body LFP reconstruction. A) Each LFP was measured over 10 trials. The data is trimmed to show from 1s before the odor pulse to 5s after its termination. B) A more detailed view showing the change in oscillation that occurs at odor onset. C) The oscillations are turned into a spectrogram, showing the power of each of the frequencies in the overall wave.

Previous research has shown that exogenous variables, such as flow rate, and humidity can affect the activity of receptor neurons and even electronic chemical sensors [18]–[23]. However, whether the sensory neuron activity is manipulated to engage or disengage adaptive gain control mechanisms in the following circuits is yet to be understood. It is possible that the magnitude of the stimulus-evoked response in the receptor neurons, their spontaneous activity, or a combination of these factors can change how information about a chemical cue is processed downstream.

In order to examine the effects of flow rate and humidity on the first-order neurons, and the resulting changes in the downstream circuit, I observed the activity in four levels of the olfactory pathway (ORNs, whole antenna, PNs and the mushroom body). Starting with the whole antenna, I examined whether flow rate or humidity level have any effect on the ability to sense an odor. Looking at the individual ORNs will allow to determine whether or not any differences in whole antenna response are the result of the summation of effects at the sensilla level, or from outside factors. Finally, examining the PN and mushroom body response will answer the question of whether or not the differences at the antenna are passed along to the brain. In all discussed levels of olfaction, I will observe the response latency of the respective cells (or whole antenna). For the PNs, ORNs and whole antenna, I will also study the magnitude of response; while for the mushroom body, I will examine the peak frequency in response to odor stimulus.

In the analysis done here, I have shown that both flow rate and humidity modulation have an effect on the response magnitude in lower-order neurons and the whole antenna. At these primary levels of the olfactory system, however, only humidity, elicited changes to the baseline activity. The resulting disparity in the effects of the downstream processing (i.e., in the locust brain) gives insight into the roles of ORN baseline activity in olfactory processing.

Chapter 2 Methods & Materials

2.1 Experimental Setups

2.1.1 Flow System

Air from a central line was passed through an activated charcoal filter to remove contaminants and a desiccant to remove moisture. This airflow was split into two streams; one stream was passed directly through to the locust; the other was diverted through a bubbler filled with water to humidify the air. Air passing through the bubbler was assumed to be saturated with water (100%RH). The saturated stream was mixed with dry air and the final humidity level was controlled by the proportion of humidified and dry air directed at the experiment. The airflow rate of each stream was controlled by a flowmeter (Cole-Palmer: 03229-10 & PMR1-010346). Two parameters were modulated in our experiments: humidity levels and background flowrates. For humidity modulation experiments, the net airflow was always 750sccm. In flow modulation experiments, the flow meter directed to the bubbler was completely closed. The lack of any bubbles in the bubbler provided evidence that no air was passing through. The needle valve on the flow meter used for the dry air was adjusted to the desired flow rates.

2.1.2 Odor Delivery

For experiments looking at changes in humidity, 1% (vol/vol) odor solutions of hexanol, isoamyl acetate (IAA) and 1-octanol were used. For experiments examining the effects of changes in flow rate, 0.5%, 1% and 2% (vol/vol) solutions of hexanol were used. The odors were diluted into 20mL of mineral oil, mixed and kept in 60 mL bottles, leaving a headspace of approximately 40mL. A pneumatic picopump (WPI, PV-280) was used for the odor delivery, injecting the odor into the delivery air at 100sccm. This pump was controlled by a LabView program that dictated the opening and closing times. When the pump was open, the air would flow into the headspace of these bottles. Odor delivery was the same throughout all experiments. The picopump was calibrated each day. Each odor puff came 10 seconds into a 30 second trial, and persisted for 4 seconds. This stimulation protocol was maintained across trials in all experimental setups.

2.1.3 Olfactory Receptor Neuron Recordings

Each locust had its legs removed and the resulting cuts sealed with VetBond (3M). The locust was then secured in a modified 6mL syringe body so that only its head was exposed. The locust head was further secured with batik wax preventing it from moving. A setup was designed to hold the syringe body and align the antenna to be secured in soft wax. A shallow cut was made in the wax, using a razor blade. This cut allowed for the constant position of the antenna to be ensured, and also maintained exposed antenna area to allow access for the incoming air and odorant. Silver chloride wires were used for the ground and lead electrodes. The ground electrode was placed inside the contralateral eye of the antenna used for measurements. A glass pipette was used as a recording electrode to probe the sensilla. This pipette was pulled using Sutter P-1000 micropipette puller to obtain an impedance on the order of 1-10MΩ. The pipette was filled with locust saline[1]. The pipette holds the lead electrode and allows for placement at individual sensilla using a Sutter MP285 micromanipulator, while observing through a microscope. Signal from the electrode then passed through an amplifier, which was set to have a high-pass filter of 300Hz, a low-pass filter of 10kHz, and a gain of 10k. This signal was recorded using a custom LabVIEW program at 15kHz.

2.1.4 Electroantennogram Recordings

A manifold and cap were designed and 3D printed specifically for these electroantennogram (EAG) recordings (Figure 2.1). This manifold allowed for airflow to be directly to the antenna, and eliminate outside air from interfering with the measurements. Intact locusts were secured, in a modified 6mL syringe body. The same syringe body was used for both ORN and EAG recordings. As in the ORN recordings, the head was stabilized using an electrowaxer. The syringe body was placed inside the EAG manifold and secured (and made air tight) using clay. With just the locust's head exposed, the antenna was extended to a well in the manifold. The antenna was kept in place using soft wax. The very tip of the antenna (i.e., the last antenna segment) was cut off so as to expose the inside of the antenna to the well. The ground electrode was placed in the contralateral eye to the antenna used for the readings. The lead

[1] Bulk locust saline composition: NaCl (1M), KCl (1M), $MgCl_2$ (1M), $CaCl_2$ (1M), $NaHCO_3$ (0.5M), Hepes (6g), Glucose (7.2g), Trehalose (15.14g), Sucrose (48g)

electrode was placed in a small hole in the bottom of the antenna well. The well was filled with locust saline to allow for electrical conductivity between the antenna and the electrode. The manifold was covered with its cap and sealed with soft wax. The cap has an inlet for the air, marked with ink to maintain a constant distance to the antenna in each experiment. Data was collected in a LabView program written to record the voltage readings at 15kHz.

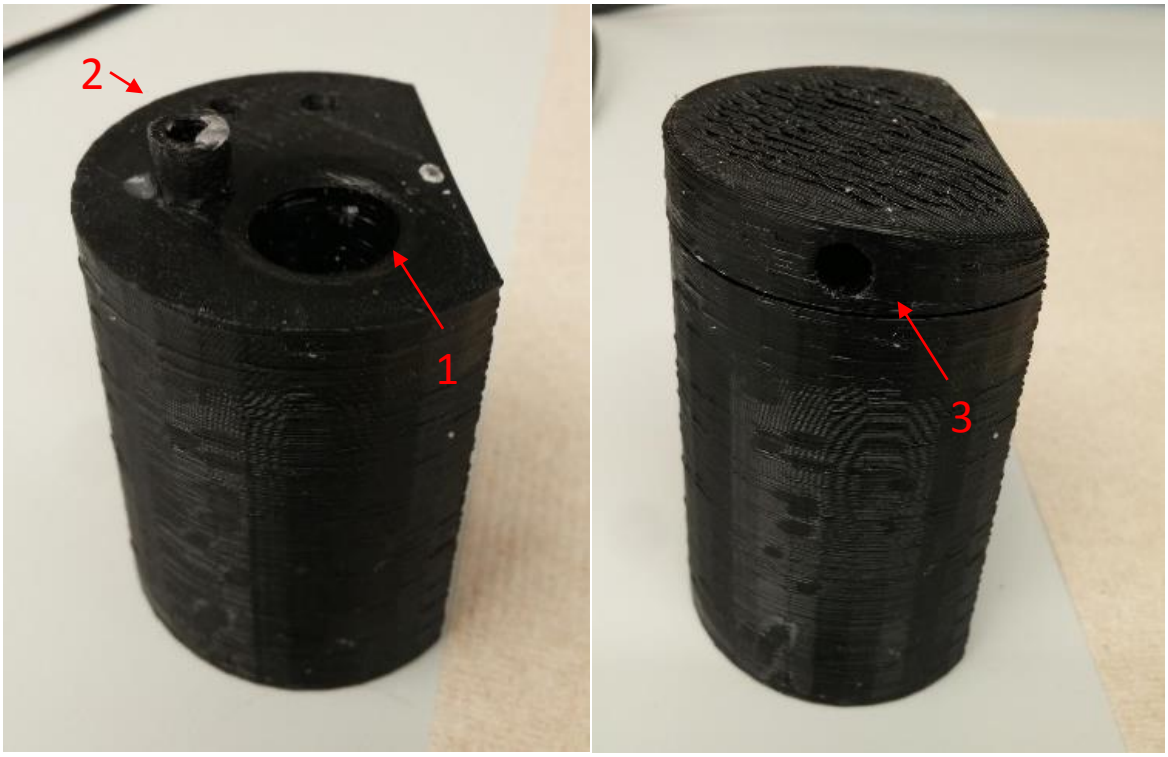

Figure 2.1: EAG Manifold. The manifold designed to maximize replicability between EAG recordings with and without the cap. 1: Opening for locust head. 2: Saline well to allow for electrical contact between the antenna and the lead electrode. 3: Air inlet in cap.

2.1.5 Central Circuit Recordings

Preparations for PN and mushroom body recordings follow the process described in previous publications [12], [24]. As in the ORN recordings, locusts had their legs removed, and the cuts were sealed with VetBond. After this, the locust was secured with electrical tape to a platform designed to consistently align the locusts in a position allowing the brain to be exposed. After this, the antenna is threaded through small tubing to expose a maximum amount, and still protect the antenna for the next step. A watertight wax cup is built around the head to allow for saline perfusion of the brain. After the cup's construction, a window is cut in the head, between the eyes, to expose the brain. In order to help eliminate potential noise sources, the gut is removed by cutting through the esophagus and pulling the entire gut out through a posterior cut in the locust. String is tied tightly around the locust anterior to the second cut to prevent saline leaks. Protease treatment allows for the brain to be desheathed, after which it is raised on a platform to expose the appropriate areas. Electrodes are placed in the mushroom body (for the LFP recordings) and the antennal lobe (for the projection neuron recordings). In PN recordings, the data was passed through an amplifier with a gain of 10k, a high-pass filter of 300Hz, and a low-pass filter of 6kHz. The readings from the mushroom body were passed through an amplifier with the same gain, 10k, a high-pass filter of 3Hz and a low-pass filter of 300Hz (these were further filtered with high- and low-pass filters of 10Hz and 50Hz, respectively).

2.2 Data Processing

2.2.1 General

Aside from spike sorting (discussed below), all data processing and figures were generated using MATLAB. Where relevant, unless otherwise stated, data is presented as mean ± SEM.

2.2.2 Normalization & Baseline Adjustments

Data normalization was performed for most experiments. In the humidity experiments, data was normalized to the first tests with dry air; whereas in the flow experiments, data was normalized to the 750sccm, 1% hexanol test. These were chosen as the tests to normalize to

because they are the most widely used and studied measurements. It followed logically to use them as the base for normalization. Where used, baseline adjustments were made by taking the reading (spike frequency, oscillatory behavior, or voltage readings) of the first nine seconds. The average of these nine seconds was then subtracted from the whole trial to adjust the initial baseline to center around zero.

2.2.3 Spike Sorting

In ORN and PN experiments, data was passed through the program Igor in order to sort the spikes from the data. From the voltage data collected, Igor is capable of distinguishing multiple cells in a single recording, and noting when these cells experience an action potential. Generating a model of the cells was designed to maximize the number of cells, while maximizing the statistical confidence that the cells were actually unique. After generating this model from three initial trials, the rest of the trials in a given experiment are fitted to the model. The final result was a list of each cell's spikes throughout each experiment.

2.2.4 PSTH Generation

In order to convert the spike raster plots into a PSTH figure, each experiment was split into time bins of 100ms (for ORN recordings) or 75ms (for PN recordings). The number of spikes in each time bin was summed. After averaging across the trials in each experiment (5 in ORN recordings, 10 in PN recordings), the newly generated PSTH was then smoothed using MATLAB's smooth function. This function smoothes the data across the nearest ten points. Smoothing was performed to remove jitter that made the figures difficult to interpret.

Chapter 3 Results of Flow Modulation

In ORN and whole antenna experiments, measurements were made at flow rates of 200, 375, 500, 750, 1000, 1500, and 2000sccm. In PN and KC experiments, these were subselected down to 375, 750 and 1500sccm. All data is normalized to results at 750sccm to allow for comparisons across conditions and experiments. For ease of reference, a data summary for the whole antenna, ORNs and PNs can be found in Table 3.2, at the end of this chapter.

3.1 Whole Antenna

Previously, to obtain an EAG, most researchers would place the tip of the antenna in a glass micro-electrode filled with locust saline that was connected to the lead electrode [25]–[27]. In the experiments presented here, the locust was placed in a manifold, with the tip of the antenna placed in a well filled with locust saline (see Methods). This proved to be quite robust, consistent between locusts, and stable over long periods.

Using the normalized data the whole antenna magnitude of responses to the flow rate changes in the EAG seem to support the initial hypothesis: as flow rate increases, the (baseline-subtracted) magnitude of the whole antenna response decreases (Figure 3.1). This trend is especially evident in the case of the 0.5% hexanol experiments. From the data in Figure 4, we can see that the normalized response magnitude decreases by approximately 38%, 30%, and 43% when the flow rate was increased from 200sccm to 2000sccm in the 2%, 1%, and 0.5% hexanol concentrations, respectively. This is relatively intuitive; increases in the flow rate mean the same amount of odor is diffused in a greater amount of carrier gas. Therefore, the antenna receives a lower concentration of odor, resulting in a weaker response. As expected, as the concentration of hexanol increases, the response magnitude at each respective flow rate increases. It appears that these concentration changes had minimal effects on the relationship between flow rate and the response magnitude.

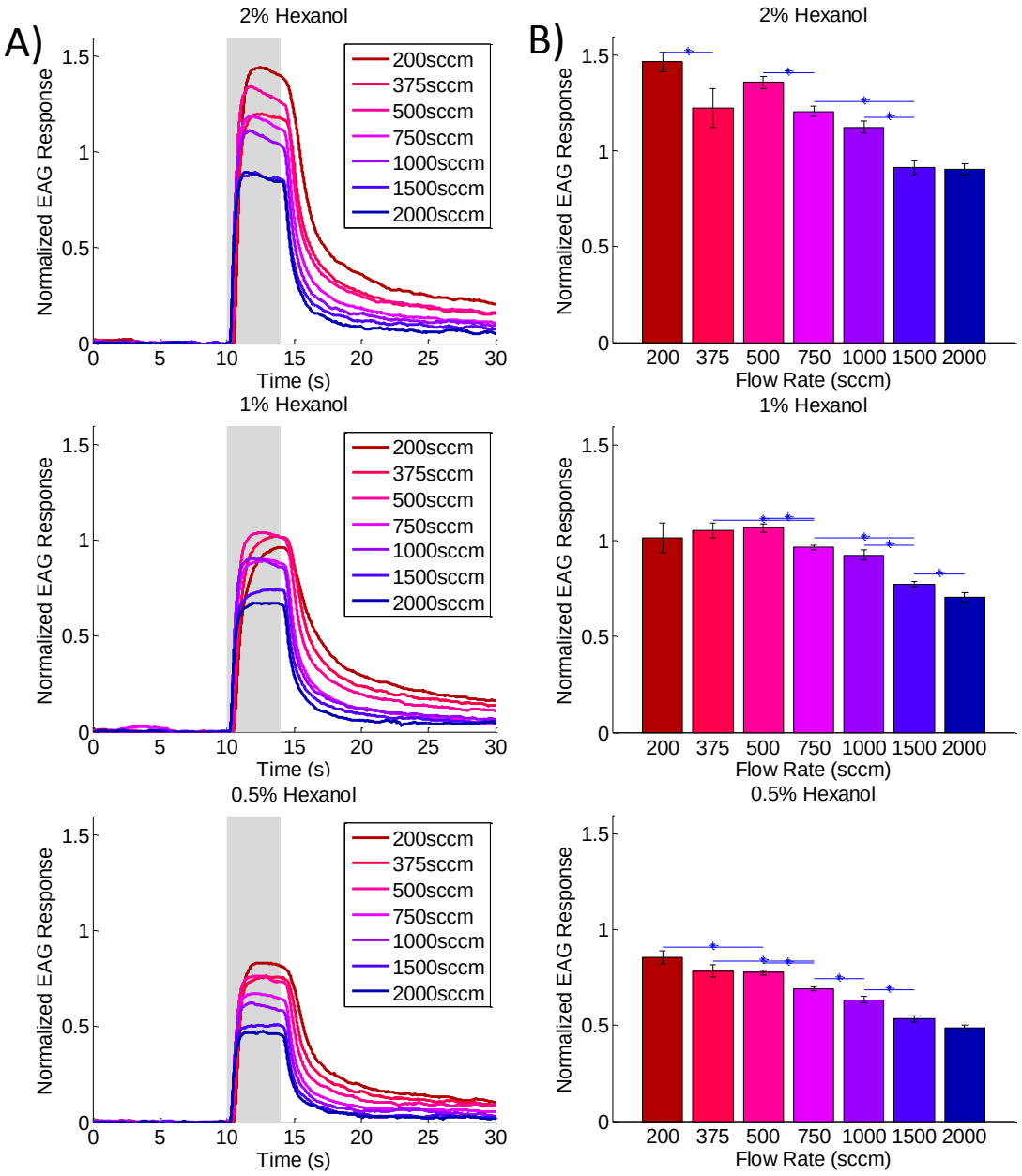

Figure 3.1: Flow rate increases cause decreased response amplitude in whole antenna. A) Mean traces of EAGs for 2%, 1% and 0.5% hexanol concentrations. B) Response amplitude, measured as the maximum voltage deflection achieved. Amplitudes decrease from 1.4656 ± 0.0509, 1.0161 ± 0.0771, and 0.8571 ± 0.0341 at a flow rate of 200sccm to 0.9037 ± 0.0277, 0.7059 ± 0.0232, and 0.4876 ± 0.0162 when flow increased from 200scccm to 2000sccm in the 2%, 1%, and 0.5% hexanol concentrations, respectively. (Mean ± SEM)

In this analysis, the response times in these experiments were affected by outliers. As such, medians were used, rather than means. Similar to the response magnitudes, the response onset time (as determined by the peak of the second derivative of the raw signal) are compared to that of 750sccm for each respective odor concentration. When compared in this manner, we see the expected trend arise: slower flow rates clearly result in a slower response in the antenna (data not shown). Interestingly, in all odor concentrations, the relative response onset seemed to reach a plateau when the flow rate was approximately 1000sccm. Moreover, the deviation from baseline as flow rate decreases seems to be greater in the 0.5% hexanol concentration. At 200sccm, for example, we see relative response times of 0.307s ± 0.04, 0.295s ± 0.476, and .364s ± 0.0933 in 2%, 1%, and 0.5% hexanol concentrations, respectively (median ± SEM). At 2000sccm, on the other hand, the relative response times are decreased to -0.178s ± 0.0552, -0.085s ± 0.3154, and 0.0137s ± 0.51, in 2%, 1%, and 0.5% hexanol concentrations, respectively (median ± SEM). The higher absolute value of plateau at higher odor concentrations is particularly interesting. This seems to indicate that the plateaus do not reflect a saturation of the receptor neurons on the antenna. Rather, we are maximizing the amount of odor being presented to the antenna.

While the response magnitude and response time were both affected by flow rate changes, the baseline voltage of the whole antenna remained relatively unchanged (Figure 3.2). Here, data is presented as the difference in voltage from the first experiments run, which were always in the 750sccm condition. Across the whole range of flows tested, though not perfectly consistent, there was no correlation between flow rate and the whole antenna baseline voltage. This data dictates that, in the whole antenna experiments, the only change in electrical signal related to flow rate is the change in response magnitude. Additionally, it supports the fact that we have not changed the baseline in such a way that the odor-induced responses are saturating the signal at a given flow rate.

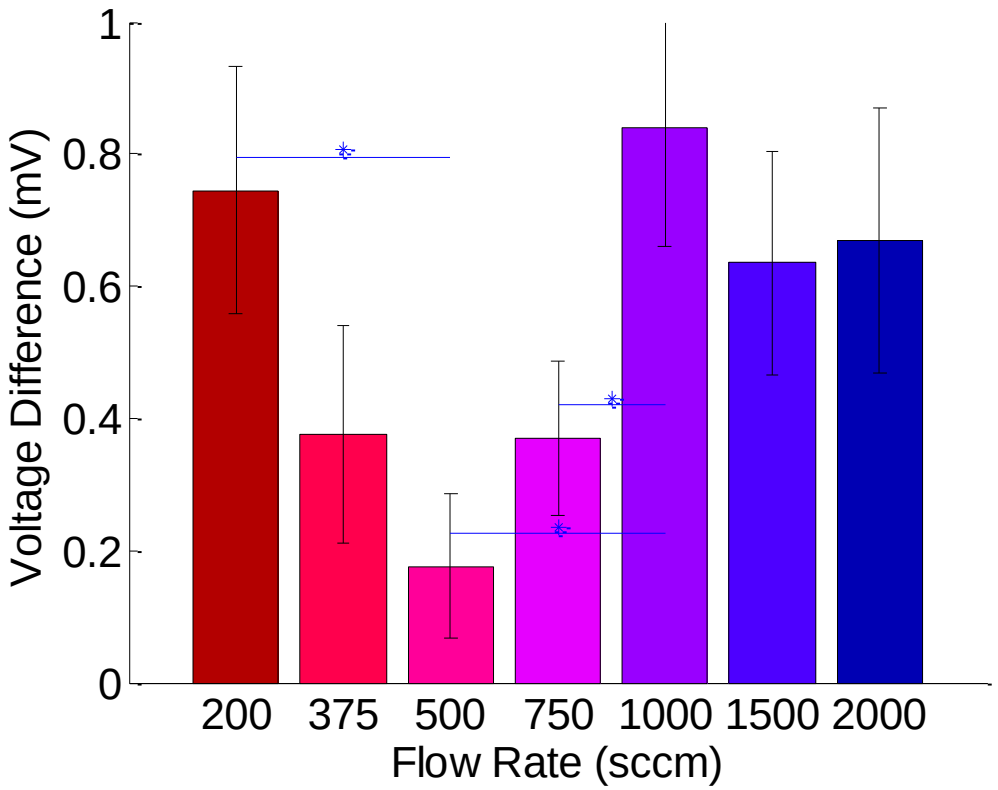

Figure 3.2: Changes in flow do not characterize baseline voltage in the whole antenna. As flow rate increases, baseline voltage does not change in a correlated manner. Data is presented as differences from the voltage of the first 750sccm tests done in each locust. Baseline voltages ranged from a minimum of 0.1764 ± 0.1082 at 500sccm to a maximum of 0.8407 ± 0.1809 at 1000sccm. (Mean ± SEM)

3.2 Olfactory Receptor Neurons

In the flow experiments, it seems that the distinct majority of sensilla had the same response pattern; therefore, summary PSTH traces of the response are appropriate representations (Figure 3.3A). In these traces, the baseline firing rate of each sensilla is subtracted to give an initial average of zero. Changes from this baseline activity, such as the increased firing rate caused by odor stimulation, are reflected as deviations away from the x-axis. In this section, when magnitude is discussed, it is presented as the average number of action potentials, or "spikes", occurring in a given 75ms time bin. Interestingly, looking at the whole population, there does not seem to be as strong of a relationship between the flow rate and the magnitude of the ORN response as we saw in the whole antenna results. Though it is only statistically significant in the 0.5% hexanol tests, the trend in all three concentrations seems to indicate a lower response magnitude as the flow increases above 750sccm (Figure 3.3B). Additionally, the plateau that we saw in the EAG readings showing that response magnitude did not decrease further at flow rates above 1000sccm is not present in the ORN readings. In fact, a plateau on the slower flow rates seems more noticeable in these experiments. As the flow rate decreases below 750sccm, the magnitude does not increase significantly. It is possible that the ORNs selected were simply tuned for detecting lower odorant concentrations, allowing them to detect hexanol in a higher flow rate. Concerns regarding under-sampling are discussed in greater depth in the Conclusion chapter. Location of sensilla on the antenna was varied, so it is unlikely that there was any antennal segment bias. Still, the general trend, coupled with the significant data from the whole antenna, supports the idea that higher flow rates cause a lower response magnitude.

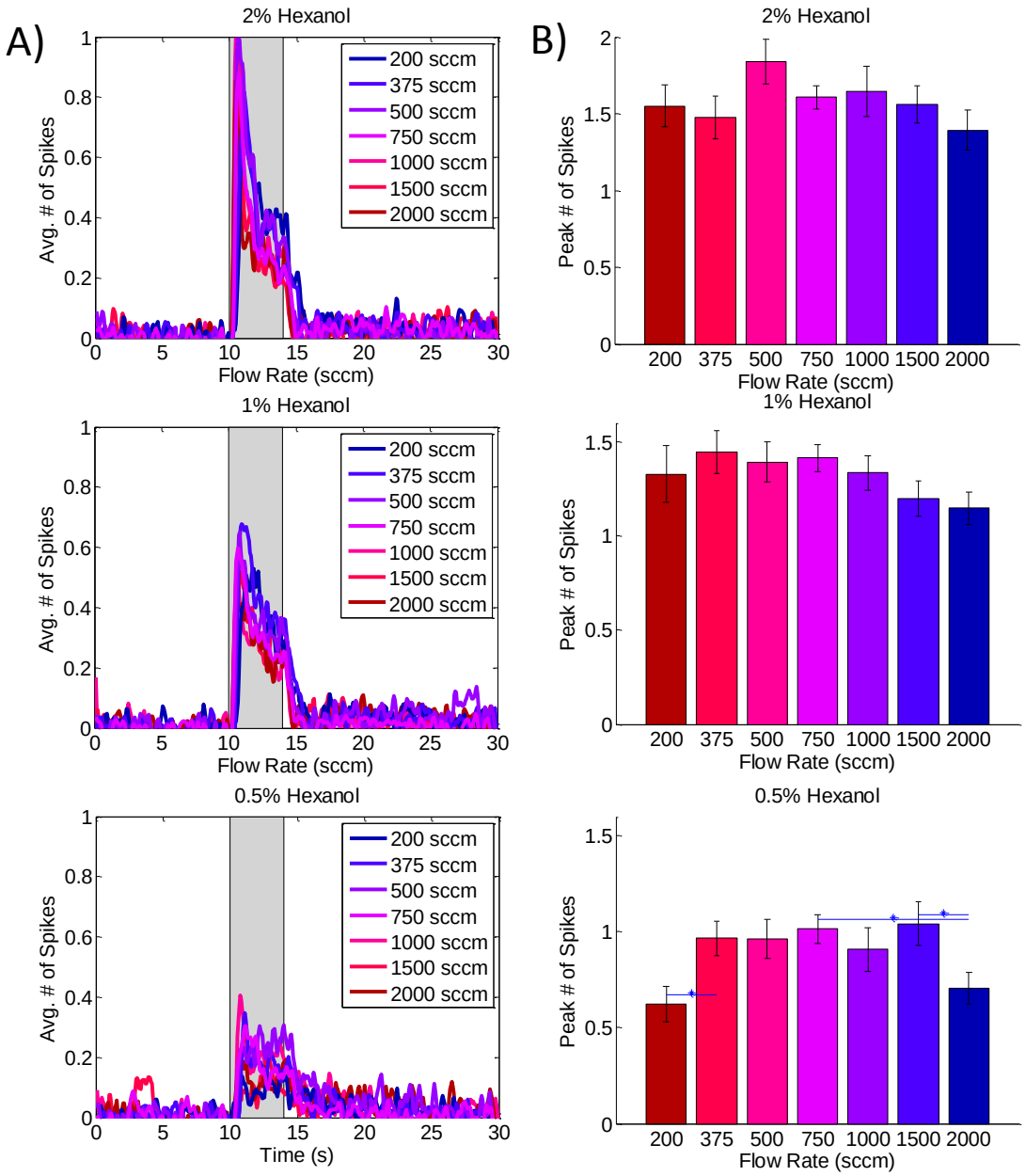

Figure 3.3: Flow rate increases do not cause significant change in ORN response amplitude. A) Mean traces of the PSTH in ORNs for three hexanol concentrations. B) Response amplitude, measured as the maximum value achieved in the PSTH analysis. None of the odor concentrations showed significant trends associated with flow rate changes. (Mean ± SEM)

As shown in Figure 3.4, the flow rate did have the expected effect on response time, i.e., the response latency decreased as the flow rate increased. This is especially evident when looking at the medians: when flow was changed from 200sccm to 2000sccm, there was a median increase in relative response time of 0.6150s, 0.3150s, and 0.8850s when the flow is reduced to 90% of its original value for 2%, 1% and 0.5% hexanol concentrations, respectively. It is interesting to note that the ORNs did not seem to exhibit the same sort of plateau behavior that the whole antenna showed as the flow rate was increased to its maximum tested value.

To further support the claim that the ORNs are truly representative of the whole antenna response, the neurons did not exhibit any change in baseline firing rate as the flow rates changed (Figure 3.5). Indeed, the population data indicates that the ORNs were even less affected by alterations to the flow rate than the whole antenna. Again, we have shown that the only changes in electrical signal caused by flow rate modulations pertain to the response magnitude.

Figure 3.4: Increased flow rates seem to decrease ORN response times. Response times for ORNs, measured by the time at which the second derivative of the PSTH curve is at a maximum. Data is normalized to 750sccm as a standard and presented as the difference (in s) from this value. In all three odor concentrations, increased flow rates seems to decrease the response time. Stars denote statistical significance ($p = 0.05$). $n = 15$. (Median ± SEM)

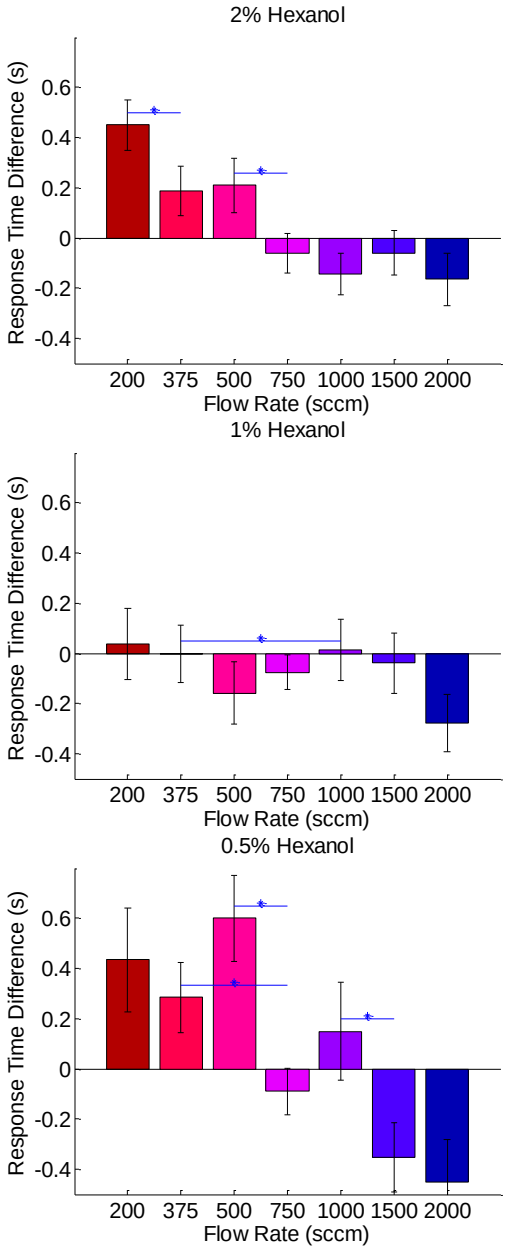

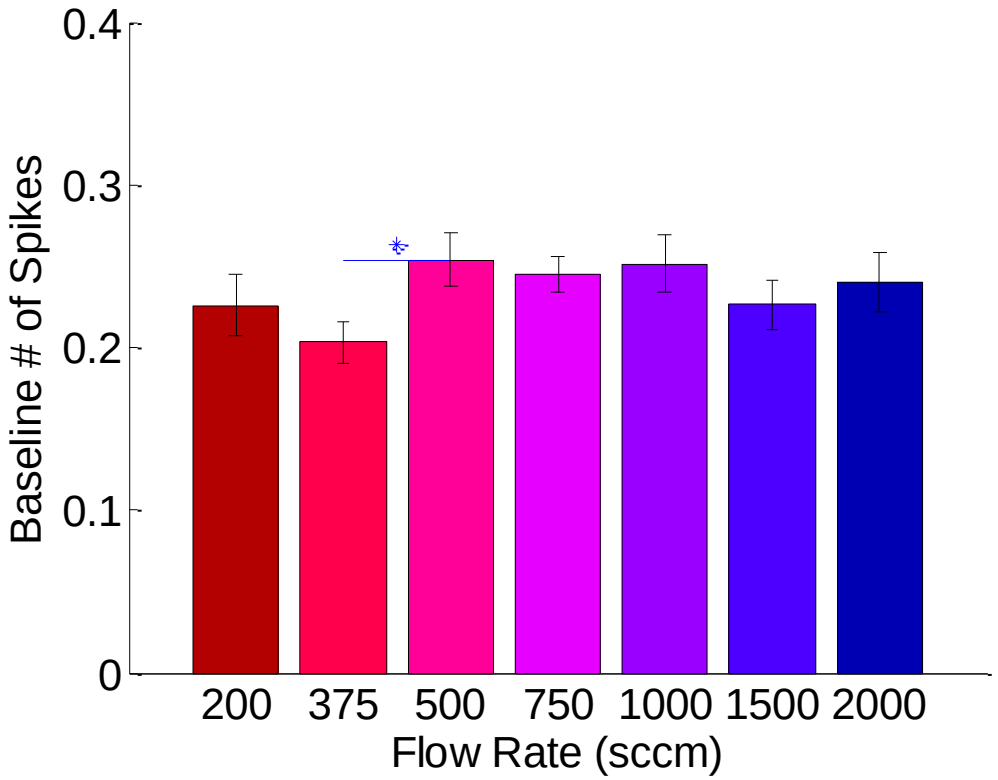

Figure 3.5: Flow rate modulation has no effect on baseline ORN activity. Changes in flow rate have virtually no effect on the spontaneous baseline activity of ORNs. The activity is almost equal throughout all flow rates tested. (Mean ± SEM)

3.3 Projection Neurons

Unlike the ORNs and whole antenna, flow rate changes had very little effect on PN responses. When flow was increased from 375sccm to 1500sccm, a 4x increase in flow rate, the average baseline activity exhibited an insignificant reduction in average spike number from 0.1834 ± 0.0069 to 0.1688 ± 0.078. In fact, the only statistically significant change in the analysis of the PNs' responses to flow rate changes came in the 1% hexanol experiments. In this case, the peak response magnitude at 375sccm was 1.2957 ± 0.0477, while at 750sccm it was merely 1.1186 ± 0.0558 (Figure 3.6A&B).

Fascinatingly, this lack of relationship to flow rate even extends into the response time. Neither mean nor median analyses indicated that there was any relationship between the flow rate and the response time. This is particularly strange, especially considering that we have now seen that the response times in ORNs and whole antenna are both affected by flow rate changes. Explanations concerning the seeming disconnect between the PNs and the ORNs are examined in greater detail in the Discussion section.

The PNs continue to prove themselves robust to flow rate modulation by maintaining the same baseline activity across all flows tested (Figure 3.7). In fact, the level of baseline activity is nearly identical across these flow rates that vary by up to 400%. At this stage, it seems that changes in flow rate no longer have an effect on the output of the neurons in the olfactory system.

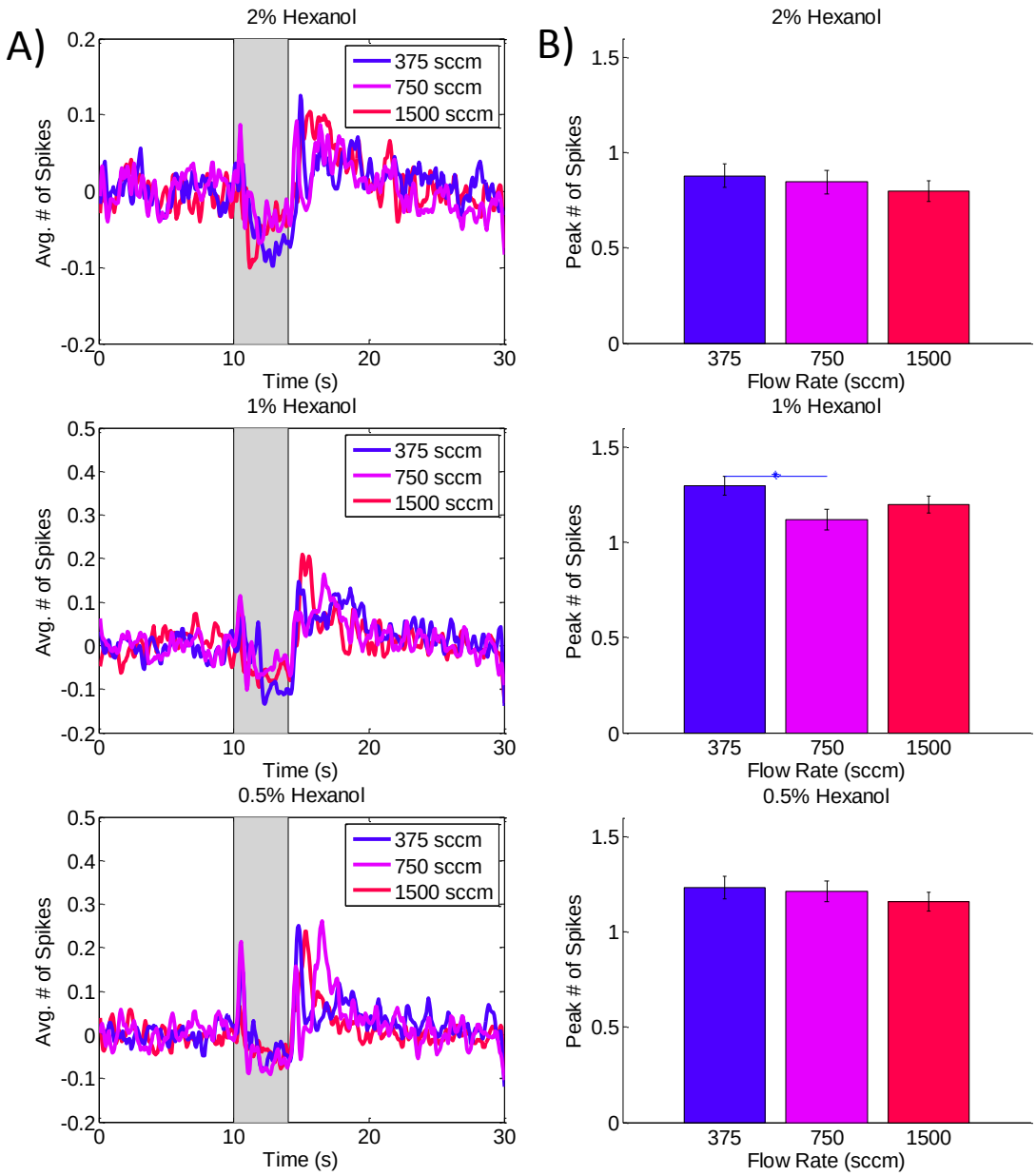

Figure 3.6: Flow rate changes do not cause significant change in PN response amplitude. A) Mean traces of the PSTH in PNs for three hexanol concentrations. B) Response amplitude, measured as the maximum value achieved in the PSTH analysis. None of the odor concentrations showed significant trends associated with flow rate changes. (Mean ± SEM)

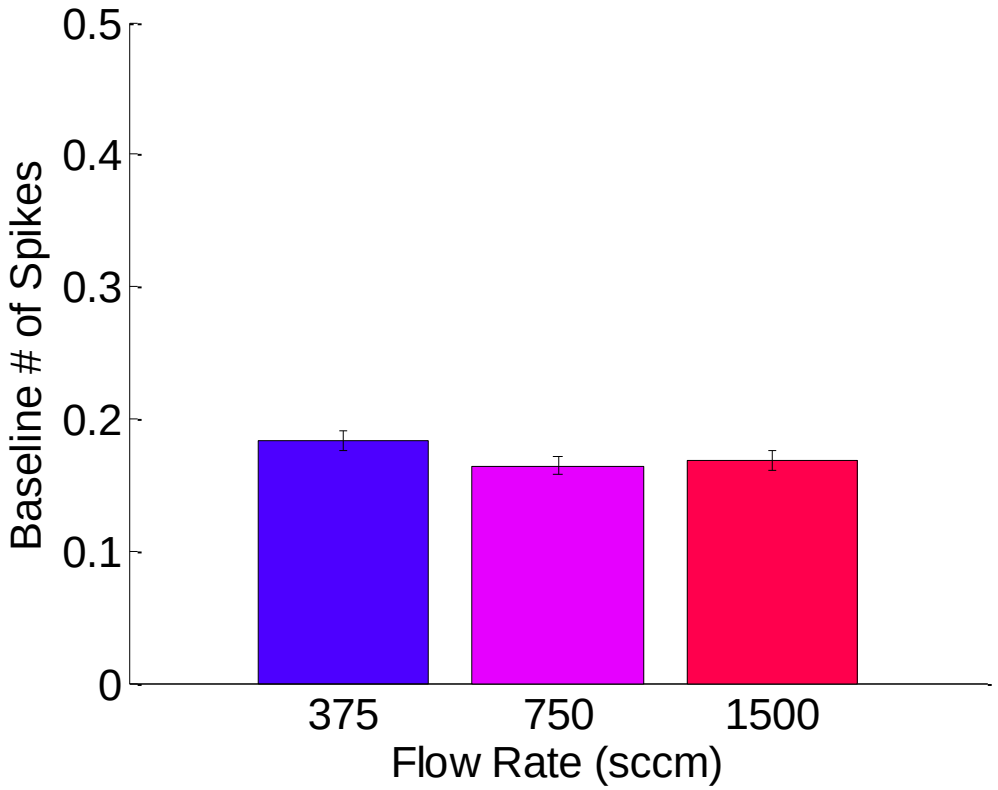

Figure 3.7: Flow rate modulation has no effect on baseline PN activity. Increasing the flow rate from 375sccm to 1500sccm causes no significant effect in the baseline spiking activity. Baseline activity was calculated as the following: 0.1834 ± 0.0069, 0.1647 ± 0.0070 , and 0.1688 ± 0.0078 , for 375sccm, 750sccm, and 1500sccm, respectively. (Mean ± SEM)

3.4 Mushroom Body

Flow rate modulation of the oscillatory neuron activity in the mushroom body revealed some correlation between cellular activity and flow rate. In order to quantitatively evaluate these effects of changes in flow rate on the oscillations, the spectrograms were converted into 2D plots by evaluating the maximum power and frequency in each time bin, averaged across trials, as shown in Figure 3.8. Different trends came through at each of the different hexanol concentrations. For example, the difference in peak power only showed significant changes in the 2% odor concentration experiments. In this case, the mean peak power of the 1500sccm (0.6122 ± 0.0421) was significantly lower than that of both 750sccm and 375sccm (0.9175 ± 0.0544 and 1.0754 ± 0.0419, respectively), as shown in Figure 3.9A. The peak powers at flows of 375sccm and 750sccm were not significantly different from one another. This decrease in power at higher flow rates for 2% hexanol is interesting, as it indicates a potential disruption in the synchronicity of the antennal lobe signal. Parallels could be drawn between these results and previous work done in moths, where high flow rates succeeded in eliminating the oscillations entirely. It should be noted, however, that there were no significant changes in the pre-stimulus oscillations at any flow rate.

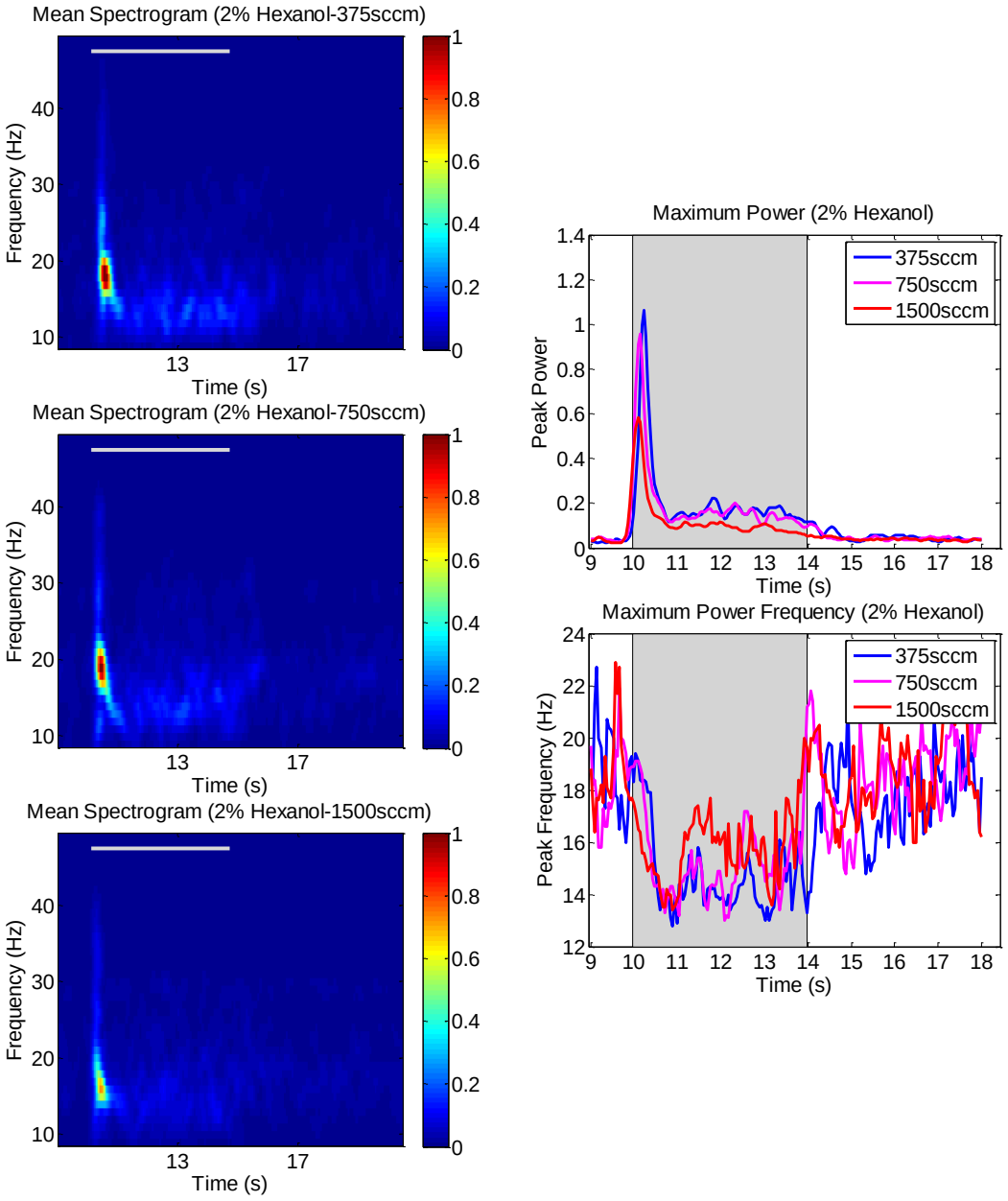

Figure 3.8: Conversion from spectrogram to 2D plots. A) Spectrograms of three flow rates (375sccm, 750sccm, and 1500sccm) when stimulated with 2% hexanol. Data is trimmed to represent 1s before the odor onset to 5s after the conclusion of the odor pulse. B) 2D plots from spectrogram data. Top Panel: peak power in each time bin. Bottom Panel: frequency that generates this peak power.

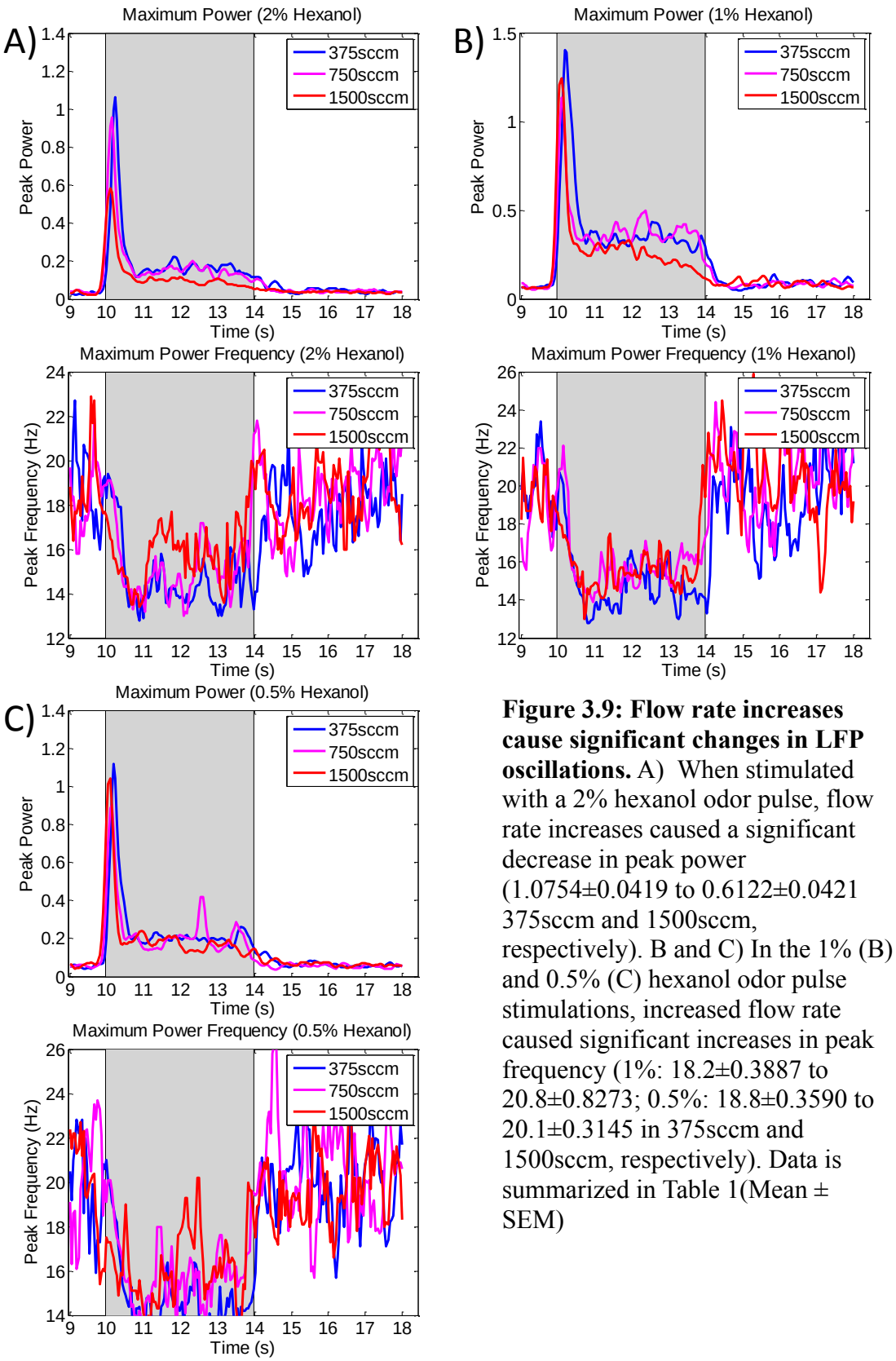

Figure 3.9: Flow rate increases cause significant changes in LFP oscillations. A) When stimulated with a 2% hexanol odor pulse, flow rate increases caused a significant decrease in peak power (1.0754±0.0419 to 0.6122±0.0421 375sccm and 1500sccm, respectively). B and C) In the 1% (B) and 0.5% (C) hexanol odor pulse stimulations, increased flow rate caused significant increases in peak frequency (1%: 18.2±0.3887 to 20.8±0.8273; 0.5%: 18.8±0.3590 to 20.1±0.3145 in 375sccm and 1500sccm, respectively). Data is summarized in Table 1(Mean ± SEM)

In all three hexanol concentrations, there was a substantial decrease in the peak frequency as flow rate increased. When increasing the flow from 375sccm to 1500sccm, the peak frequency decreased nearly 2Hz when stimulated with 2% hexanol (Figure 3.9A), while in the 1% and 0.5% hexanol conditions, the peak frequency decreased approximately 0.7Hz and 1.60Hz, respectively (Figure 3.9B&C). Neither condition seems to have a linear relationship between flow rate and peak frequency. Interestingly, however, it appears that the threshold for significant decreases in frequencies is different between the various conditions. In the 2% concentration, the peak frequency in the 1500sccm flow rate tests was significantly lower than that of both of the other flow rates. In the 1% and 0.5% tests, however, the 1500sccm peak frequency was only significantly different from the peak frequency at 750sccm and 375sccm, respectively. Additionally, in all three conditions, as may be expected, the time of the peak frequency was significantly reduced at a flow rate of 1500sccm, compared to 375sccm. Time to the maximum value was reduced by approximately 0.13s, 0.2s and 0.12s in 2%, 1%, and 0.5% hexanol concentrations, respectively. Data from the LFP analyses are summarized below, in Table 3.1.

Hexanol Concentration	Flow Rate (sccm)	Norm Peak Power	Peak Time (s)	Peak Frequency (Hz)
2%	*375*	1.0754±0.0419	10.4084±0.0094	18.3000±0.2603
	750	0.9715±0.0544	10.2984±0.0131	19.000±0.4472
	1500	0.6122±0.0421	10.2723±0.0157	16.40±0.2603
1%	*375*	1.4838±0.1133	10.4031±0.0188	18.2±0.3887
	750	1.2679±0.1472	10.6335±0.2829	20.3±0.7753
	1500	1.3432±0.0834	10.2513±0.0165	17.50±0.5821
0.05%	*375*	1.139±0.0739	10.3665±0.0105	18.8±0.3590
	750	1.0218±0.1719	10.8272±0.0122	18.1±1.1494
	1500	1.0818±0.1384	10.2461±0.3631	17.20±0.3887

Table 3.1: Summary of LFP flow rate results. Red boxes indicate significant results. In the 2% hexanol concentration, normalized peak power was significantly reduced at higher flow rates. Both 1% and 0.5% hexanol concentrations showed significant increases in peak frequency as flow rate increased. (Mean ± SEM)

It can now be said that although flow rate causes changes in the response magnitude of lower-order neurons. This change, however, does not elicit a characteristic effect in the response of the PNs. Moreover, we can confidently say that none of the significant results are the caused by changes in the time constants of the neuron responses, as we do not see changes in the response times of the PNs, nor in the synchronicity, as represented by the LFP results.

Whole Antenna		**2% Hexanol**	**1% Hexanol**	**0.5% Hexanol**	
	Flow Rate (sccm)	**Mean Normalized EAG Response**	**Mean Normalized EAG Response**	**Mean Normalized EAG Response**	**Baseline EAG Voltage**
	200	1.4656 ± 0.0509	1.0161 ± 0.0771	0.8571 ± 0.0341	0.7455 ± 0.1882
	375	1.224 ± 0.1013	1.0558 ± 0.0381	0.7844 ± .0316	0.3757 ± 0.1644
	500	1.3576 ± 0.0308	1.0685 ± 0.0214	0.7767 ± 0.0117	0.1764 ± 0.1082
	750	1.2059 ± 0.0273	0.9666 ± 0.0118	0.6919 ± 0.0106	0.348 ± 0.1138
	1000	1.1242 ± 0.0319	0.9256 ± 0.0255	0.6341 ± 0.0156	0.8407 ± 0.1809
	1500	0.9124 ± 0.0354	0.7744 ± 0.0155	0.5345 ± 0.0174	0.6348 ± 0.1695
	2000	0.9037 ± 0.027	0.7059 ± 0.0232	0.4867 ± 0.0162	0.6689 ± 0.2003
ORN		**2% Hexanol**	**1% Hexanol**	**0.5% Hexanol**	
	Flow Rate (sccm)	**Peak Spike Count**	**Peak Spike Count**	**Peak Spike Count**	**Baseline Spike Count**
	200	1.551 ± 0.1379	1.326 ± 0.1507	0.6229 ± 0.0905	0.226 ± 0.0190
	375	1.4758 ± 0.1416	1.4453 ± 0.1140	0.965 ± 0.0887	0.2032 ± 0.0127
	500	1.8392 ± 0.1428	1.3905 ± 0.1061	0.9624 ± 0.0995	0.2541 ± 0.0166
	750	1.6068 ± 0.0745	1.4124 ± 0.0694	1.10145 ± 0.0743	0.245 ± 0.0114
	100	1.6461 ± 0.1627	1.3342 ± 0.0907	0.9073 ± 0.1131	0.2515 ± 0.0177
	1500	1.5608 ± 0.1235	1.1968 ± 0.0943	1.0405 ± 0.1140	0.2266 ± 0.0151
	2000	1.3912 ± 0.1305	1.1468 ± 0.0872	0.7049 ± 0.0842	0.2406 ± 0.0183
PN		**2% Hexanol**	**1% Hexanol**	**0.5% Hexanol**	
	Flow Rate (sccm)	**Peak Spike Count**	**Peak Spike Count**	**Peak Spike Count**	**Baseline Spike Count**
	375	0.8788 ± 0.0602	1.2957 ± 0.0477	1.2325 ± 0.0572	0.1834 ± 0.0069
	750	0.8454 ± 0.0630	1.1186 ± 0.0558	1.2121 ± 0.0560	0.1647 ± 0.0070
	1500	0.7972 ± 0.0535	1.1987 ± 0.0450	1.1567 ± 0.0500	0.1688 ± 0.0078

Table 3.2: Summary of results of flow modulation experiments for whole antenna, ORNs and PNs.

Chapter 4 Results of Humidity Modulation

The relative humidity of the carrier gas was varied to four different levels for testing (100% relative humidity (RH) air, 66% RH air, 33% RH, and 100% dry air), and was tested in three odors (hexanol, iso-amyl acetate (IAA), and 1-octanol) as described in Methods. As with flow, the whole antenna, ORN and PN data is summarized in Table 4.2, at the end of this chapter. In all experiments, the first and last set of trials were both in dry air to ensure any changes in response magnitude were not the result of signal degradation. Where relevant, all trials were normalized to the mean of the initial dry trials.

4.1 Whole Antenna

The changes in carrier gas humidity seemed to have different effects on each odor's response. In Figure 4.1, we see baseline-adjusted values in order to evaluate the magnitude of the antenna response. In hexanol, as the level of humidity increases, the normalized response magnitude decreases in a seemingly linear fashion. Each successive level of humidity is significantly different from one another. The normalized hexanol response magnitude decreased by over 12% as humidity was increased from 0%RH to 100%RH. Unlike the graded humidity-magnitude relationship observed in hexanol, 1-octanol, only showed a significant change between dry air and the first humidity level (1.0272 ± 0.0107 in 100% dry air, compared to 0.9835 ± 0.0187 in 33%RH air). Once any humidity was added, none of the responses were significantly different from one another. Finally, IAA had a similar step-like response as 1-octanol, but required a higher level of humidity to produce a significant magnitude decrease. The first significant difference from dry air in response magnitude for these experiments occurred at 66%RH. Here, we see normalized response magnitudes of 1.0537 ± 0.0136 and 0.9872 ± 0.0333, respectively. One might expect that humidity would act either in a step-wise fashion to decrease the magnitude, or as a switch. Given the data, it seems that humidity has the potential to act in either of these mechanisms, depending on which odor is used as the stimulus.

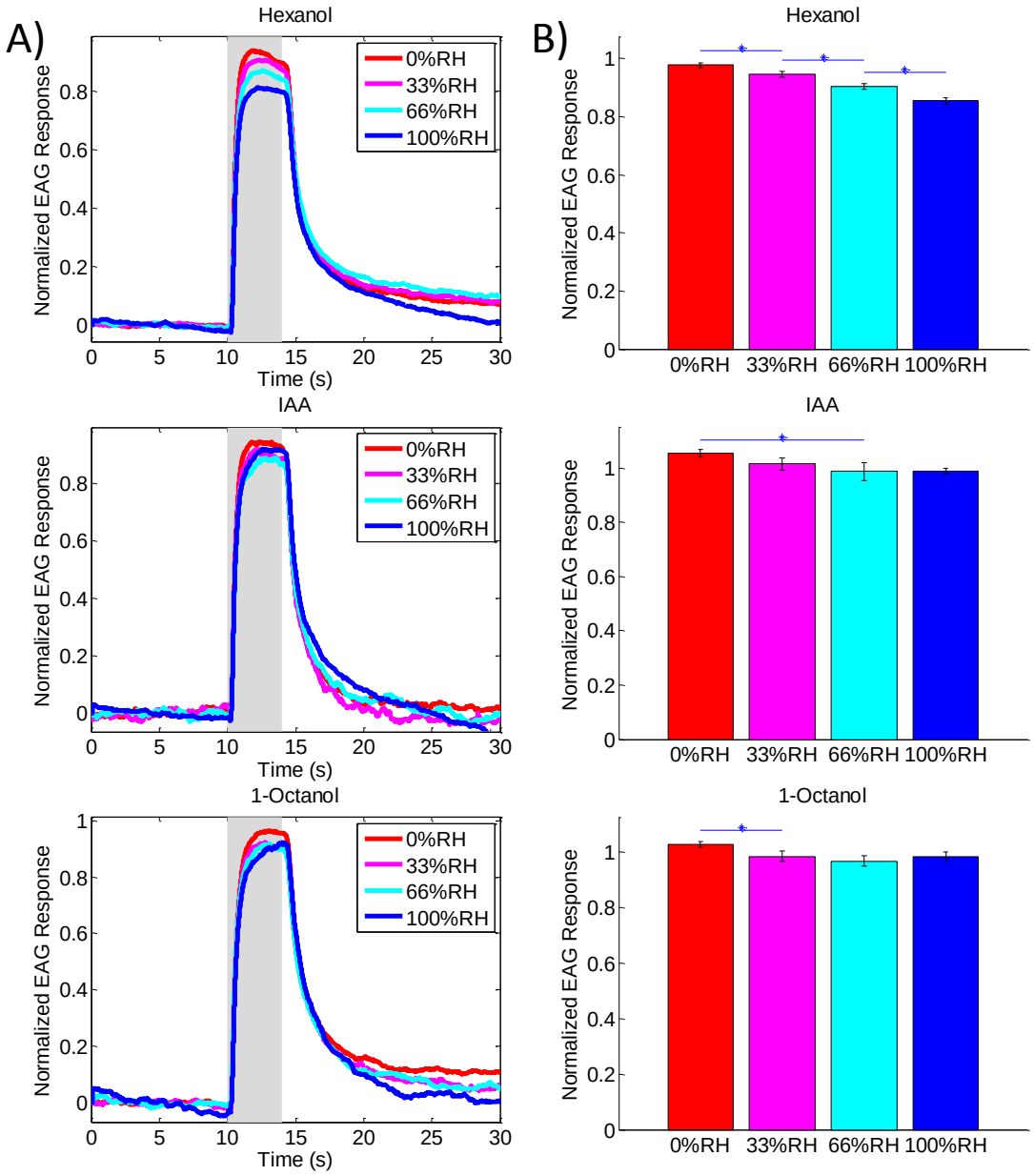

Figure 4.1: Humidity increases cause decreased response amplitude in whole antenna. A) Mean traces of EAGs for hexanol, IAA and 1-octanol odor stimulations. B) Response amplitude for all three odors, measured as the maximum voltage deflection achieved. Data is normalized to the initial 0%RH test. Amplitudes decrease from 0.9776 ± 0.0074 to 0.8539 ± 0.0107, 1.0537 ± 0.0136 to 0.9887 ± 0.114 and 1.0272 ± 0.0107 to 0.9839 ± 0.0167, and when humidity increased from 0%RH to 100%RH in the hexanol, IAA, and 1-octanol stimulatoins, respectively. Hexanol response amplitudes demonstrated a linear relationship with humidity, while IAA and 1-octanol exhibited a step-like decrease in amplitude occurring before 66%RH and 33%RH, respectively Stars denote statistical significance (p = 0.05). n = 13. (Mean ± SEM)

Additionally, as the humidity levels were changed, the baseline voltage of the antenna changed dramatically (Figure 4.2). There was a clear and direct, linear correlation between the baseline voltage and the humidity level: as the humidity increased, the baseline voltage decreased. Setting the first dry air trial at 0V allowed for normalization. As humidity was increased from 0%RH to 100%RH, the baseline EAG voltage decreased by over 1mV. As increasing voltage corresponds to greater antenna response, the decreased voltage signifies that the baseline activity of the whole antenna is lower in more humid conditions. This brings greater meaning to the magnitude reductions, as we can now confidently state that the magnitude reduction is not merely due to increased activity causing saturation of the receptor neurons. Baseline levels typically took approximately one minute to stabilize after humidity changes (data not shown), which may indicate a progressive mechanism of more and more ORNs adjusting to the humidity changes. Dry baseline values were taken at the beginning and the end of each experiment to account for baseline drift over time. It should be noted that for the purposes of this particular analysis, data was not separated by odor, as the baseline activity is not associated with odor response.

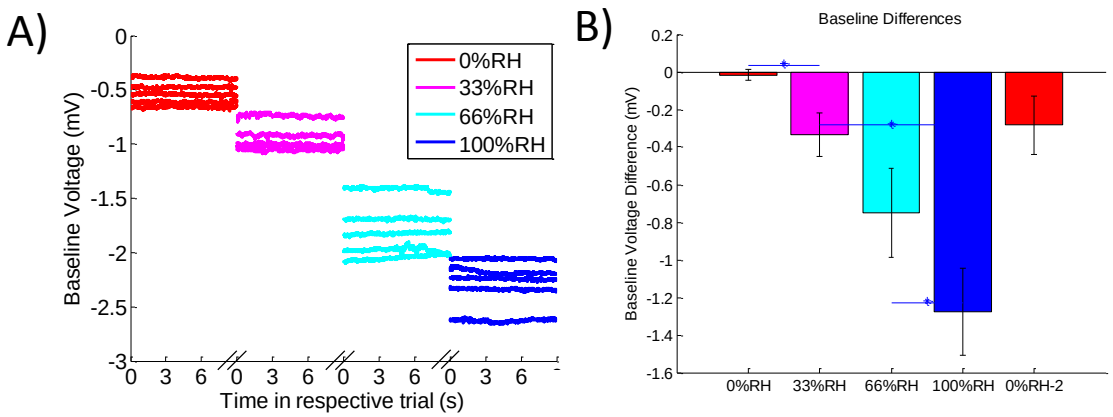

Figure 4.2: Humidity increases cause a decrease in baseline voltage in whole antenna. A) An example of raw baseline voltages from a representative EAG experiment as humidity is modulated. Each trace represents the first 9s of baseline activity before the odor pulse is given (at 10s) for a single trial at the specified humidity level. B) A representation of the mean baseline voltage difference at each humidity level. Data is presented as differences from the voltage of the initial dry test. As humidity increases, mean baseline voltage seems to decrease linearly. Baseline voltages were calculated as follows: -0.1457mV ± 0.0100, -0.3342mV ± 0.0216, -0.7509mV ± 0.0442, and -1.2539mV ± 0.0338, in 100% dry air, 33% humid air, 66% humid air, and 100% humid air, respectively. (Mean ± SEM)

As shown in Figure 4.3, the whole antenna response time to odor stimulus remained unchanged in all odors as humidity was increased. This indicates that the decrease in response magnitude is not due to the increased water molecules in the air interfering with the odorant's ability to reach the antenna. Additionally, this suggests that humidity has not altered the time constants for the odor response. As with the flow rate changes, in order to further evaluate the effects of humidity on the sensory system's response, we must look at the effect on individual ORNs.

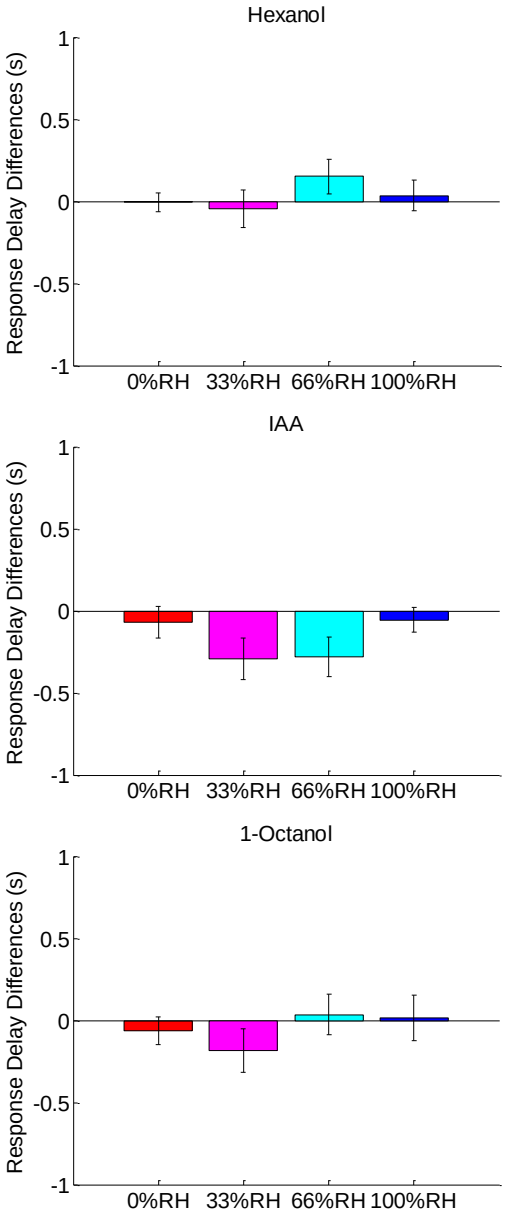

Figure 4.3: Increased humidity has no effect on whole antenna response times. Response times are presented relative to that of the initial dry experiments. Negative values imply that the response came earlier than the dry tests. In all three odors, there did not appear to be any effect as humidity was increased. n = 13. (Mean± SEM)

4.2 Olfactory Receptor Neurons

Though summary plots of the effects of humidity on ORNs (Figure 4.4) give some insight into the effects of humidity at this level, at least at the population level, it was difficult to discern any trend relating the response magnitude to the humidity level in any of the three odors tested. Only 1-octanol showed a significant decrease in average peak spike activity between the 100% dry and 100% humid conditions, where it decreased from, 1.3107 ± 0.0541in 100% dry air to 1.1473 ± 0.0590 in 100%RH air. Though not much was readily unveiled relating the response magnitude to humidity, there was a clear decrease in the baseline activity. Interestingly, though the ORNs reflected the antenna's anti-correlation with humidity, the ORNs reflected more of a switch-like behavior (Figure 4.5). Only 100% humid air, with a mean baseline spike activity of 0.1776 ± 0.0127 was significantly lower, and it was significantly different from each other condition. Here, we do not see the recovery to initial baseline activity upon returning to 0%RH. However, since we can observe this recovery in the whole antenna recordings, we can say that this discrepancy is most likely due to undersampling.

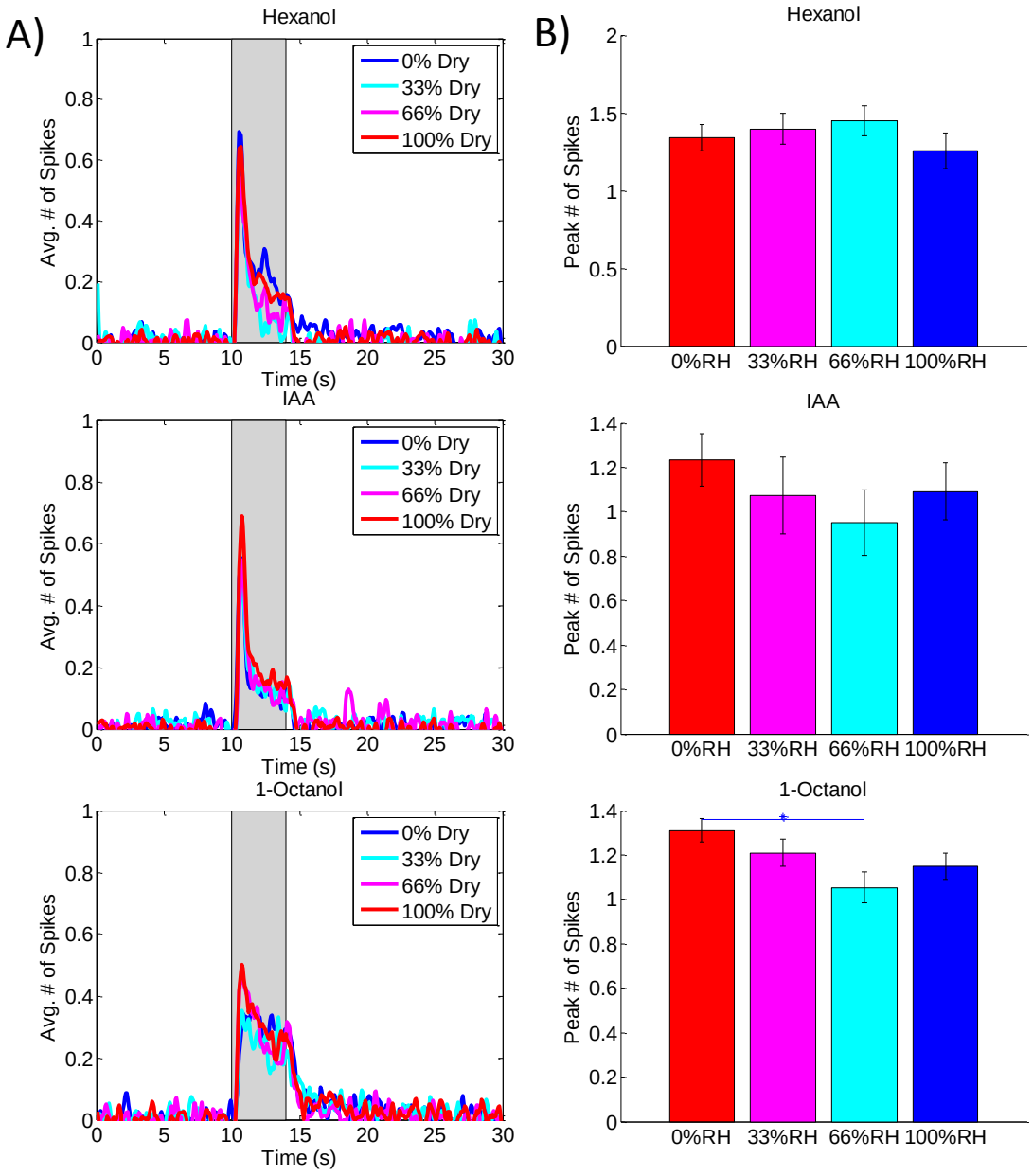

Figure 4.4: Humidity increases do not significantly effect ORN response amplitudes. As humidity increases, there was no significant trend in the response amplitude of the ORNs for any of the three odors tested. (Mean ± SEM)

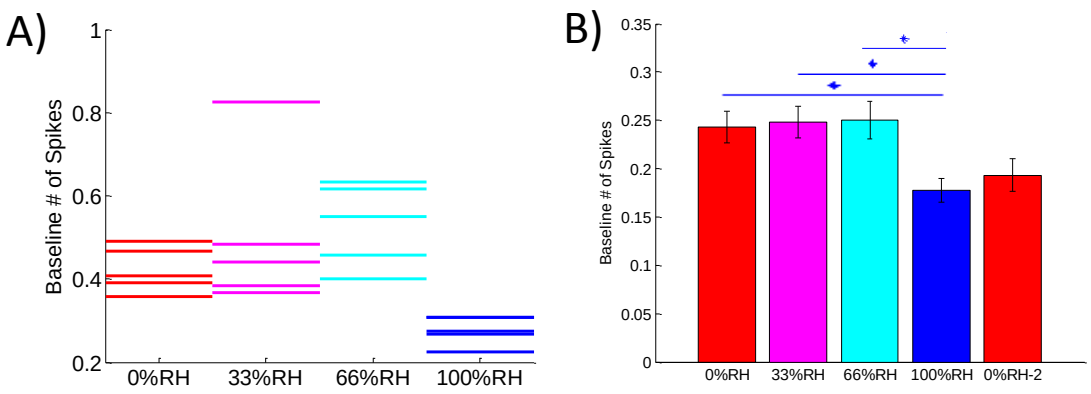

Figure 4.5: ORN baseline activity is significantly decreased in 100%RH conditions. A) An example of raw baseline data from a single ORNN as humidity is modulated. Each line represents the mean baseline spike probability of a single trial, defined as the first 9s of a trial, at the specified humidity level. B) Representation of the mean baseline spiking activity of the total ORN population at each humidity level. Mean baseline spike probabilities were calculated to be 0.2234 ± 0.0118, 0.2480 ± 0.0163, 0.2501 ± 0.190, and 0.1776 ± 0.0127, in 100% dry air, 33% humid air, 66% humid air, and 100% humid air, respectively. (Mean ± SEM)

Individual ORNs were selected for closer examination by comparing their baseline and peak magnitude spike probabilities in 100%RH and dry air conditions. Those that were significantly different in both baseline activity and peak magnitude were designated “significant” (Figure 4.6). This identification process in and of itself revealed some interesting results. There were a total of 7 neurons that had higher baseline activity in dry air, and only 5 with higher baseline activity in humid air. This matches the behavior of the whole antenna baseline, which had a drop in baseline voltage as humidity was increase. Decreased ORN firing will cause a decrease in voltage in the whole antenna. It is important to note, however, that even the “significant” magnitude responses of these ORNs did not correlate to humidity the same way as the whole antenna. All three odors exhibited more neurons with significantly higher response magnitudes in dry air condition vs the 100%RH condition (6 vs 2, 4 vs 0, and 3 vs 0 for hexanol, IAA, and 1-octanol, respectively). This is reflective of the decreased response magnitude shown in the whole antenna recordings.

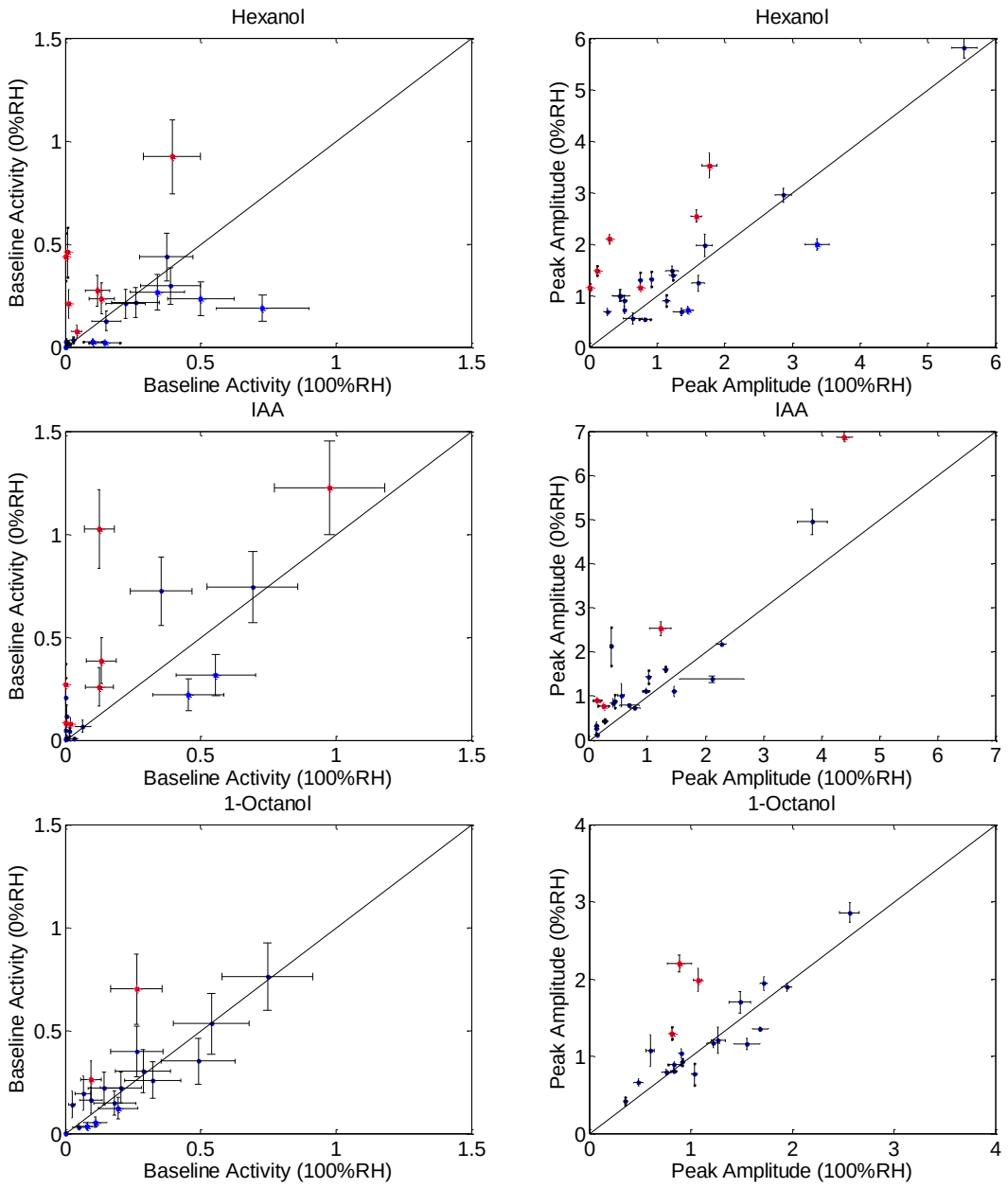

Figure 4.6: Individual ORN baseline and response amplitude comparisons. The baseline and response amplitude of each ORN is plotted to compare the values in 0%RH and 100%RH conditions. Neurons that are significantly different from the line representing unity are colored: red for those that are significantly higher in the dry condition, and blue for those that are significantly higher in the humid condition. In hexanol, 6 ORNs were more responsive in 0%RH conditions, while only 2 were more responsive in 100%RH air. In IAA and 1-octanol stimulations, no neurons showed higher responses in the 100%RH condition, while 4 and 3 neurons were more responsive in the 0%RH condition, respectively. For the baseline, 7 ORNs were more active in the dry condition, and 5 were more active in the humid condition. Stars denote statistical significance ($p = 0.05$). $n = 17$, 15 and 15, for IAA, hexanol, and 1-octanol. (Mean ± SEM)

Though the magnitude responses in the ORNs did not reflect that of the whole antenna, the time of response to odor stimulus seemed to share the antenna's lack of correlation to the level of humidity. All three odors failed to exhibit any trends related to the humidity of the carrier gas.

4.3 Projection Neurons

Population analysis of the projection neurons showed some conceivable trends in response magnitude to humidity (Figure 4.7). These results actually seem to be the opposite of what was observed in the whole antenna. Both hexanol and 1-octanol demonstrated significant increases in response magnitude between the dry air and 100%RH air conditions. When the delivery air went from dry to 100%RH, the normalized hexanol responses increased by nearly 20% from 1.1223 ± 0.0362 to 1.3130 ± 0.0678. 1-octanol changed nearly as much as between dry and humid conditions, increasing from 1.0483 ± 0.0267 to 1.2192 ± 0.0492. IAA, however, did not seem to demonstrate a consistent trend as humidity was altered.

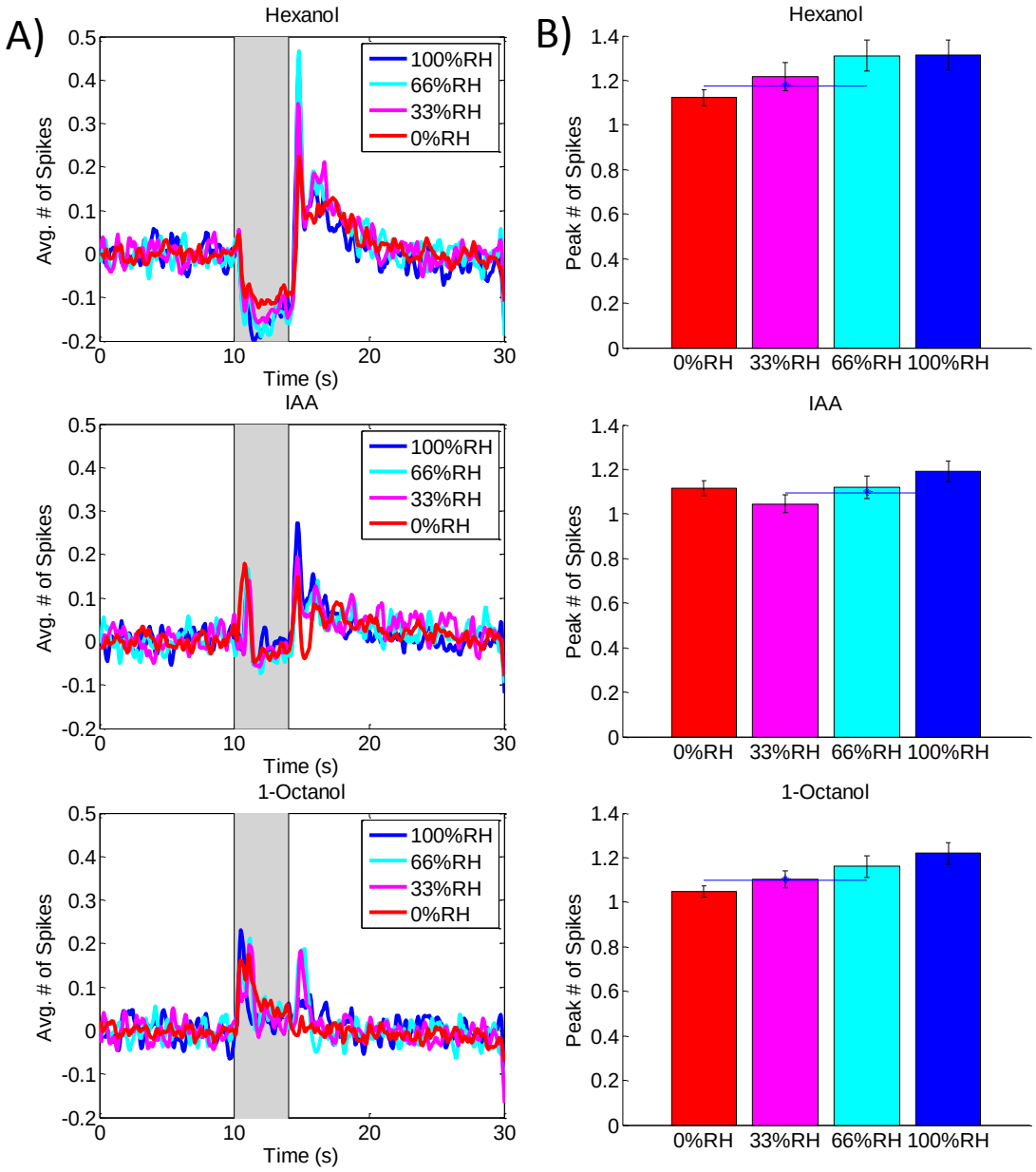

Figure 4.7: Humidity increases cause increased response amplitudes in the PN population. A) Mean traces of the PSTH in PNs for the various humidity levels in all three odors. B) Response amplitude, measured as the maximum value achieved in the PSTH analysis. In all odors, as humidity was increased, the response amplitude increased. Between the 0%RH and 100%RH conditions, response amplitudes increased from 1.1223 ± 0.0362 to 1.3130 ± 0.0678, 1.1168 ± 0.0332 to 1.1905 ± 0.0454, and 1.0483 ± 0.0267 to 1.2192 ± 0.049, for hexanol, IAA, and 1-octanol, respectively. (Mean ± SEM)

The baseline activity (Figure 4.8) of the population of PNs shows a stark linear relationship with humidity. Unexpectedly, however, the baseline activity increases significantly with each successive increase in humidity, i.e., the reverse of the ORN humidity response. From a spike average of 0.1791 ± 0. 0047 in 100% dry air, the baseline activity in the PNs increases up to 0.2360 ± 0.0072 in 100% humid air. This is the opposite effect of what we have seen thus far in ORNs and the whole antenna, where baseline activity decreased significantly in the presence of humidity. When examined individually, the data showed that 8 PNs had significantly higher baseline activity in the 100%RH air conditions, while only 1 had higher baseline activity in the dry air.

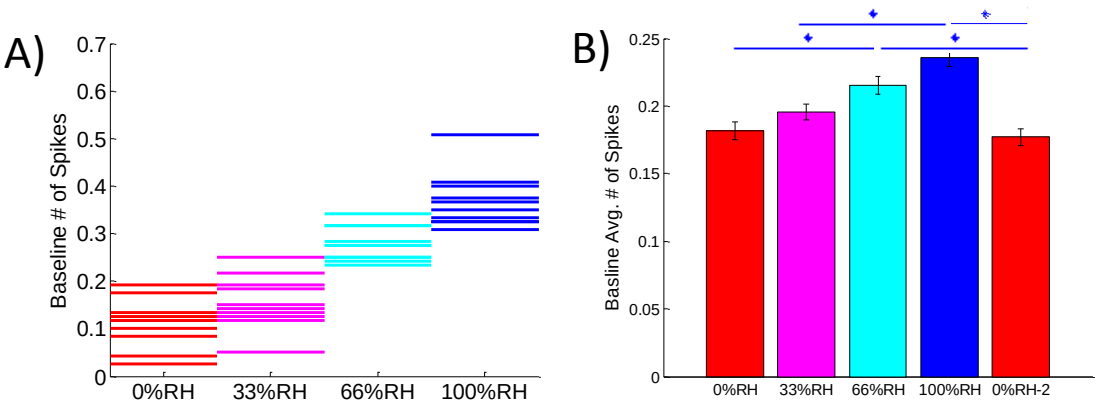

Figure 4.8: Increases in humidity cause increases in the baseline activity of PNs. A) An example of raw baseline data from a single PN as humidity is modulated. Each line represents the mean baseline spike probability of the first 9s of a single trial at the specified humidity level. B) Representation of the mean baseline spiking activity of the total PN population at each humidity level (75ms time window). Mean population baseline spike probabilities were calculated as follows: 0.1791 ± 0.0047, 0.1955 ± 0.0061, 0.2151 ± 0.0067, and 0.2360 ± 0.0072 in the 0%RH, 33%RH, 66%RH, and 100%RH conditions, respectively. (Mean ± SEM)

Additionally, though none were statistically significant, there was a potential observable effect on the response time (Figure 4.9). All three odors demonstrated a delayed response onset when the odor was delivered in humid air. Both IAA and 1-octanol showed a gradated increase in response time as %RH was increased. Hexanol on the other hand, showed no increase in response time until the air was completely humid. These observations are interesting for multiple reasons. First, there was no difference in response time for either hexanol or IAA at the whole antenna or even the ORN population level. It is surprising that such a trend would arise this late in the olfactory processing chain. Moreover, it is interesting to note that the odors exhibiting linear increases in response time as humidity was increased were the ones that showed step decreases in the response magnitude, and vice versa. However, it is clear that the error in these measurements is high enough to prevent any confident conclusions from being made.

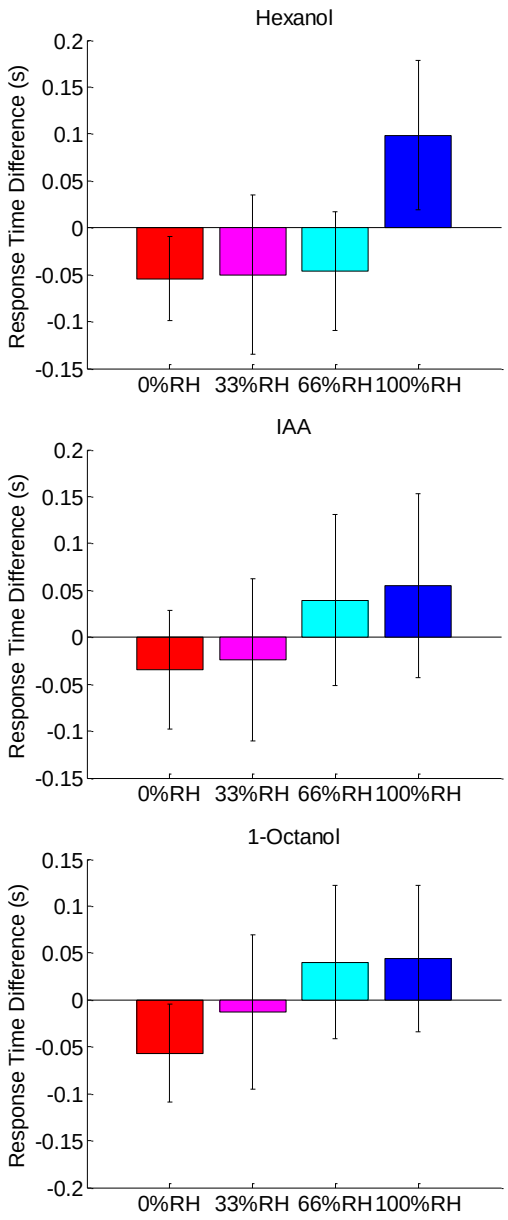

Figure 4.9: Increases in humidity seem to increase PN response times. Response times for PNs, measured by the time at which the second derivative of the PSTH curve is at a maximum. Data is normalized to the first dry run as a standard and presented as the difference (in s) from this value. Though not statistically significant, all three odors seemed to increase in response time as humidity was increased. Stars denote statistical significance ($p = 0.05$). $n = 13$. (Mean ± SEM)

In the same way that significant ORNs were identified, PNs were also analyzed to observe the amount of significant individual neurons' baseline activity and response magnitude (Figure 4.10). Interestingly, both hexanol and 1-octanol had more neurons with significantly higher response magnitudes in the 100%RH condition compared to the 0%RH condition: 5 vs 0 for hexanol, 3 vs 0, and 1-octanol. IAA, on the other hand, had 2 neurons with significantly higher response magnitudes in both 100%RH and 0%RH conditions. Additionally, in baseline conditions, 7 of these PNs had significantly higher baseline spike activity in the 100%RH condition, while only 2 neurons was significantly more active in the 0%RH condition. Once again, the activity demonstrates a reversal in humidity-related behavior from that of ORNs.

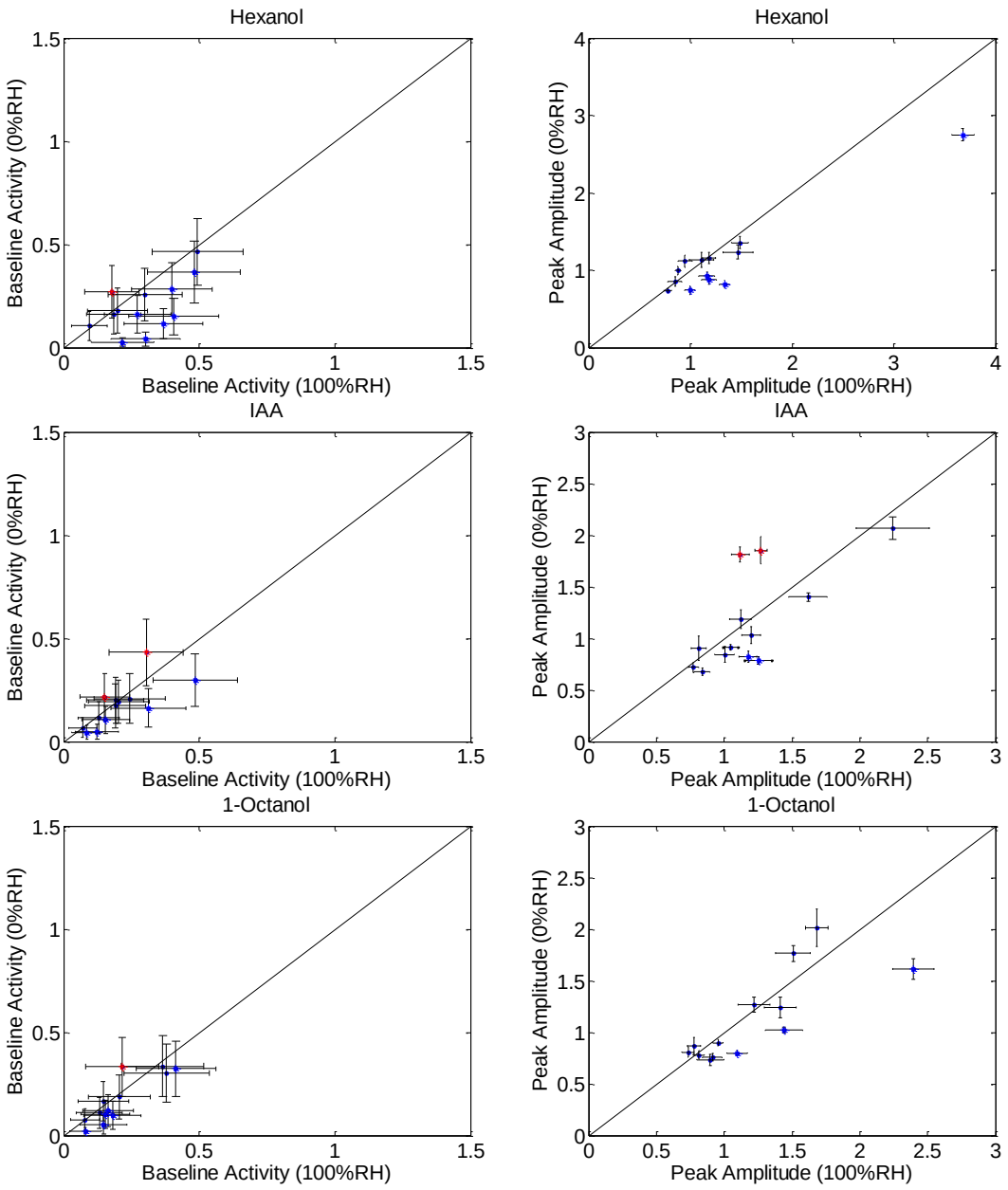

Figure 4.10: Individual PN baseline and response amplitude comparisons. The baseline and response amplitude of each PN is plotted to compare the values in 0%RH and 100%RH conditions. Neurons that are significantly different from the line representing unity are colored: red for those that are significantly higher in the dry condition, and blue for those that are significantly higher in the humid condition ($p = 0.05$). Both hexanol and 1-octanol had no neurons that had significantly higher responses in the dry condition and 9 that had higher responses in the humid condition. 2 neurons had significantly higher responses to IAA in the dry condition, while 7 had stronger responses in the humid condition. For the baseline, 37 PNs were more active in the dry condition, and 9 were more active in the humid condition. $n = 13$. (Mean ± SEM)

PNs were also examined by separating them into two groups based on their response pattern: those with a response to the odor onset, and those whose response was to the odor offset. If a neuron had both responses, it was included in both groups. Interestingly, when separated in this manner, the trend of increasing baseline activity as humidity increases seems to persist in the group with onset responses. For the onset group, there were 4 neurons with significantly higher baselines in the 100%RH air condition, while only 2 neurons had baselines in the 0%RH air condition that were significantly higher. However, we are still able to observe an increase in response magnitude in both hexanol and 1-octanol (Figure 4.11). In both these odor stimulations, the 100% dry trials had significantly lower response magnitudes than the 66%RH and 100%RH air trials. Hexanol showed a gain in response magnitude from 0.8759 ± 0.0270 to 1.0451 ± 0.0456, and 1-octanol exhibited an increase from 1.1346 ± 0.0319 to 1.3105 ± 0.0593, as the humidity rose from dry air to 100%RH air. Again, these results are contradictory to the behavior of the ORNs, which reduce their activity with increases in humidity.

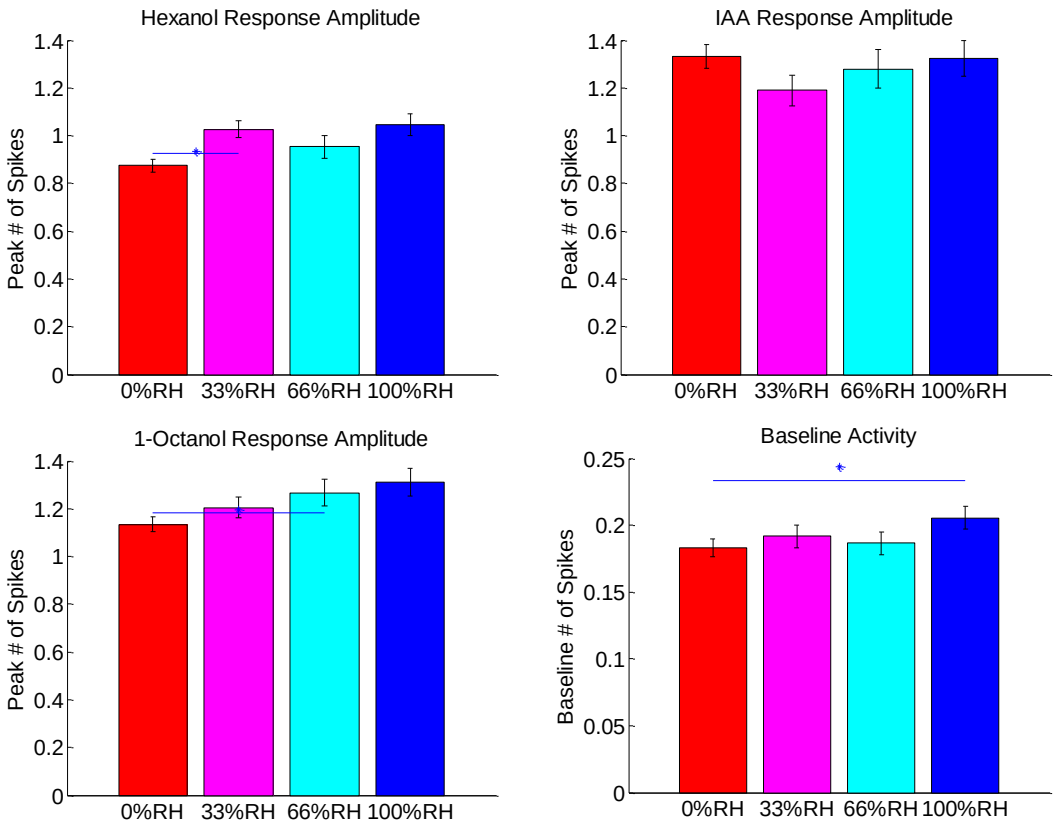

Figure 4.11: Response amplitude increases persist in the onset-responsive subset of PNs. Response amplitude, measured as the maximum value achieved in the PSTH analysis. In all odors, as humidity was increased, the response amplitude increased. Between the 0%RH and 100%RH conditions, response amplitudes increased from 0.8759 ± 0.0270 to 1.0451 ± 0.0456, 1.3317 ± 0.0507 to 1.3236 ± 0.0743, and 1.1346 ± 0.0319 to 1.3105 ± 0.0594, for hexanol, IAA, and 1-octanol, respectively. Lower right panel: Baseline activity also significantly increased as the humidity was increased. In the 0%RH conditions, the baseline spike probability was 0.1834 ± 0.0067. In the 100%RH condition, the baseline activity was significantly higher, 0.2055 ± 0.0085. (Mean ± SEM)

In the offset group, there was an even greater disparity in the amount of neurons that had significantly different baselines: 5 neurons were significantly higher in the 100%RH condition, and only 2 were significantly higher in the 100% dry condition. In fact, the mean baseline increased from 0.1934 ± 0.0061 to 0.2473 ± 0.0090 between the dry air and 100%RH air conditions. Interestingly, similar to the onset group, both hexanol and 1-octanol showed increased response magnitude with rising humidity (Figure 4.12). Hexanol response magnitudes grew from 1.2005 ± 0.0447 to 1.4342 ± 0.0839, and 1-octanol response magnitudes increased from 1.1224 ± 0.0486 to 1.3795 ± 0.1174, as humidity was increased. This could indicate a common source of input, especially due to the opposite effect of humidity on the PNs compared to the ORNs.

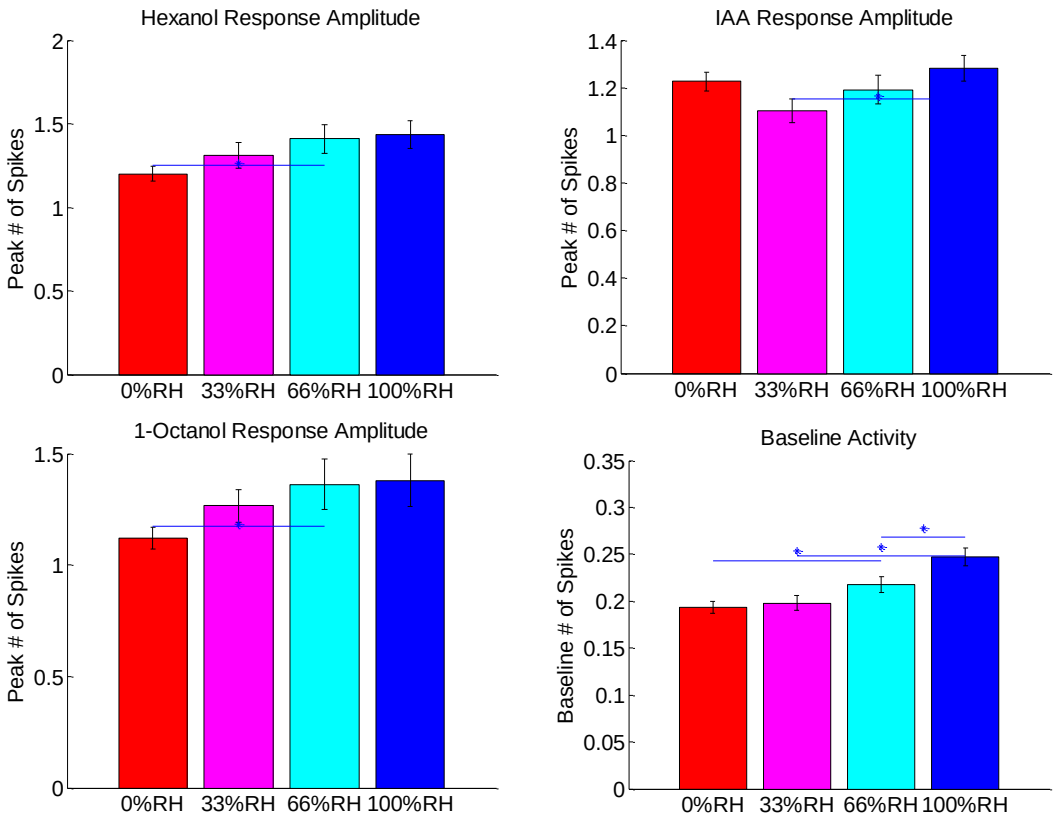

Figure 4.12: Response amplitude increases persist in the offset-responsive subset of PNs. Response amplitude, measured as the maximum value achieved in the PSTH analysis. While IAA did not show the same trend, hexanol and 1-octanol, exhibited increased response amplitude as humidity was increased. Between the 0%RH and 100%RH conditions, response amplitudes increased from 1.2005 ± 0.0447 to 1.4342 ± 0.0839, and 1.1224 ± 0.0486 to 1.3795 ± 0.1174, for hexanol, and 1-octanol, respectively. Lower right panel: Baseline activity increased in a more linear fashion than shown in the onset-responsive subset. Baseline spike probability was 0.1934 ± 0.0061, 0.1979 ± 0.0077, 0.2181 ± 0.0085, and 0.2473 ± 0.0090 in the 0%RH, 33%RH, 66%RH and 100%RH conditions, respectively. (Mean ± SEM)

4.4 Mushroom Body

As mentioned previously, the oscillatory activity in the mushroom body for the humidity modulation experiments was measured using LFPs and then transformed into spectrograms to evaluate the power of each frequency over time (Figure 4.13). Data is normalized to a single trial in the first experiment using 100% dry air. Again, higher power means the magnitude of that specific frequency in the MB oscillations was higher. It is clear from these figures that the oscillations and behavior still persist at all levels of humidity, but in order to gain a quantitative measurement, as with the flow rate experiments, the spectrograms were transformed into a two-dimensional plot by evaluating the maximum of the power at each time bin. By evaluating the value of the peak power, time at which this power occurs, and the peak frequency at this time, it is possible to compare the data from multiple humidity conditions. From these plots, we see that the presence of humidity not only maintains the steady state effects of odor stimulation, but also has minimal effects on peak power magnitude, peak frequency, and response time. Quantitative results of this analysis are summarized in Table 4.1. Although the peak frequency seems to increase slightly in the humid conditions for all odors, these results were not statistically significant. The changes in humidity seemed to have no effect on baseline oscillation frequency or power. The lack of significant results still maintains interest. We can now say with confidence that, since the LFP does not indicate any changes in the synchronicity of neuron firing, the reductions in response magnitude are not related to changes in firing rates or reaction time constants. This seems to be a characteristic of the compensatory action of the PNs in response to changes in the ORNs.

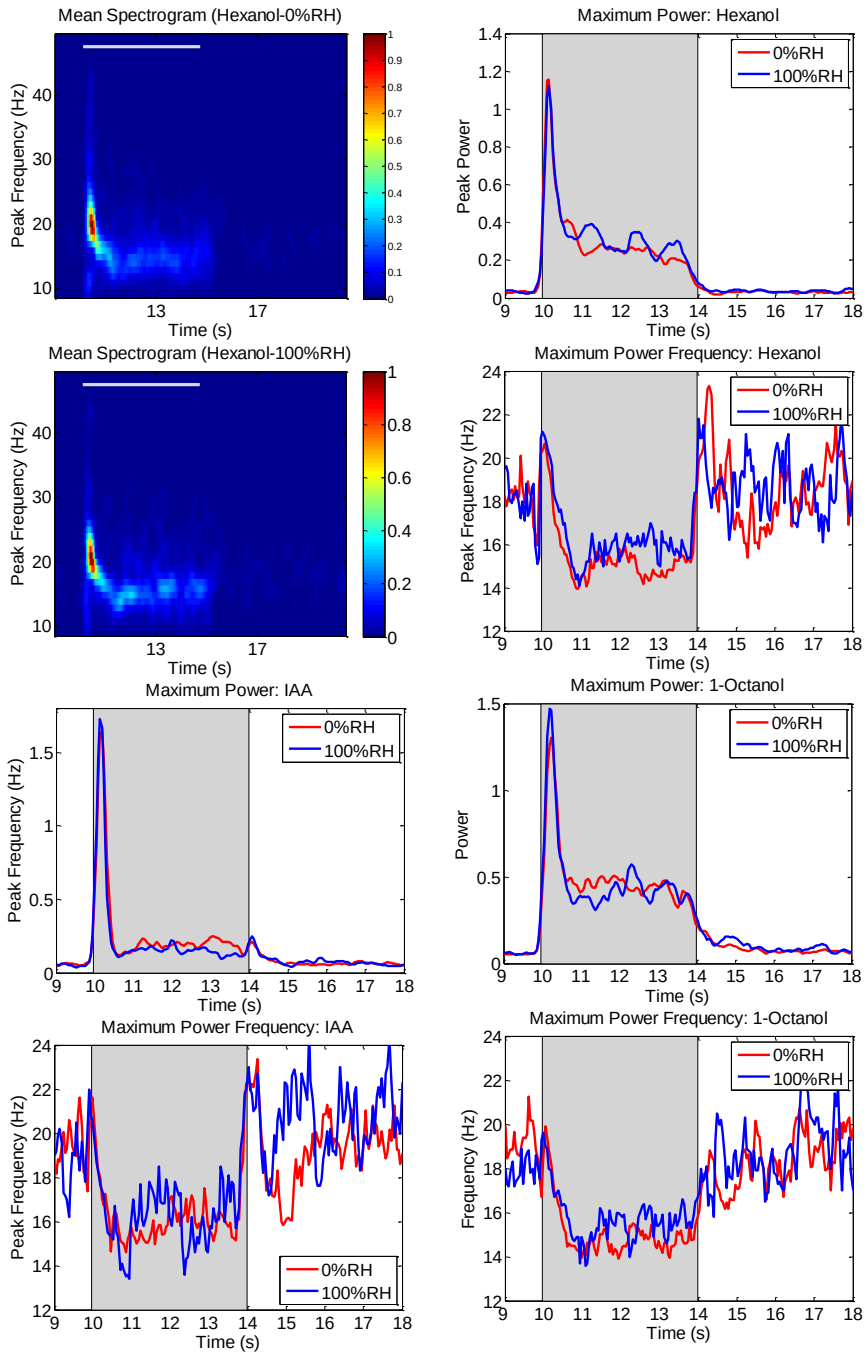

Figure 4.13: Humidity increases do not cause significant changes in LFP oscillations. A) Representative spectrograms of hexanol. Data was transformed from spectrograms to 2D plots as described previously. B-D) 2D analysis of hexanol, IAA, and 1-octanol. There were no significant changes to peak power, peak frequency or time of peak occurrence in any humidity conditions for any of the three odor stimulants. Data is summarized in Table 2 (Mean ± SEM)

Odor	Condition	Norm Peak Power	Peak Time(s)	Peak Frequency (Hz)
Hexanol	*Dry*	1.2115±0.0792	10.2958±0.0156	19.8000±0.3293
	Humid	1.1475±0.0726	10.2932±0.0080	20.5000±0.3073
IAA	*Dry*	1.7632±0.1487	10.6230±0.1984	18.0500±0.4615
	Humid	1.7662±0.1215	10.3298±0.0085	18.1±0.4333
1Octanol	*Dry*	1.4503±0.1154	10.5785±0.1281	17.0±0.3627
	Humid	1.5788±0.0801	10.3297±0.0194	17.4000±0.4000

Table 4.1: Summary of LFP humidity results. No significant changes were observed in any humidity conditions. Peak power, peak time, and peak frequency all remained constant within odors as humidity ranged from 0%RH to 100%RH. **(**Mean ± SEM)

		Hexanol	IAA	1-Octanol	
Whole Antenna	**Humidity Level**	**Mean Normalized EAG Response**	**Mean Normalized EAG Response**	**Mean Normalized EAG Response**	**Baseline EAG Voltage(mV)**
	0%RH	0.9776 ± 0.0074	1.0537 ± 0.0136	1.0272 ± 0.0107	-0.144 ± 0.0774
	33%RH	0.9453 ± 0.0101	1.0148 ± 0.0224	0.9835 ± 0.0187	-0.3342 ± 0.1165
	66%RH	0.9038 ± 0.0102	0.9872 ± 0.0333	0.9666 ± 0.0191	-0.7509 ± 0.2380
	100%RH	0.8539 ± 0.0107	0.9887 ± 0.0114	0.9839 ± 0.0167	-1.2767 ± 0.2311
		Hexanol	**IAA**	**1-Octanol**	
ORN	**Humidity Level**	**Peak Spike Count**	**Peak Spike Count**	**Peak Spike Count**	**Baseline Spike Count**
	0%RH	1.3408 ± 0.0849	1.2355 ± 0.1181	1.3107 ± 0.0541	0.2234 ± 0.0118
	33%RH	1.3951 ± 0.0994	1.0733 ± 0.1726	1.2095 ± 0.0625	0.2480 ± 0.0163
	66%RH	1.4490 ± 0.0985	0.9509 ± 0.1497	1.0540 ± 0.0700	0.2501 ± 0.0190
	100%RH	1.2560 ± 0.1123	1.0920 ± 0.1297	1.1473 ± 0.0590	0.1776 ± 0.0127
		Hexanol	**IAA**	**1-Octanol**	
PN	**Humidity Level**	**Peak Spike Count**	**Peak Spike Count**	**Peak Spike Count**	**Baseline Spike Count**
	0%RH	1.1223 ± 0.0362	1.1168 ± 0.0332	1.0483 ± 0.0267	0.1791 ± 0.0047
	33%RH	1.2160 ± 0.0627	1.0447 ± 0.0402	1.1042 ± 0.0380	0.1955 ± 0.0061
	66%RH	1.3112 ± 0.0690	1.1188 ± 0.0497	1.1597 ± 0.0472	0.2151 ± 0.0067
	100%RH	1.3130 ± 0.0678	1.1905 ± 0.0454	1.2192 ± 0.0492	0.2360 ± 0.0072

Table 4.2: Summary of results of humidity modulation experiments for whole antenna, ORNs and PNs.

Chapter 5 Conclusion

5.1 Discussion

In these experiments with flow and humidity modulation, we have seen two distinct effects on the olfactory system. In flow modulation experiments, we see that an increased flow rate caused only a decrease in response magnitude in the ORNs that was also reflected in the whole antenna recordings. These changes did not alter the behavior of the PNs, and showed minimal effects on the LFP signal in the mushroom body. In the humidity modulation experiments, however, increases in humidity levels caused not only a similar decrease in response magnitude, but also elicited a change in baseline firing activity of the ORNs, that was also reflected as a decrease in baseline voltage in the whole antenna. Unlike the flow experiments, the humidity modulation caused characteristic changes in both the response magnitude and baseline activity of the PNs, which resulted in an unaffected LFP signal in the mushroom body. These results are summarized concisely in Figure 5.1.

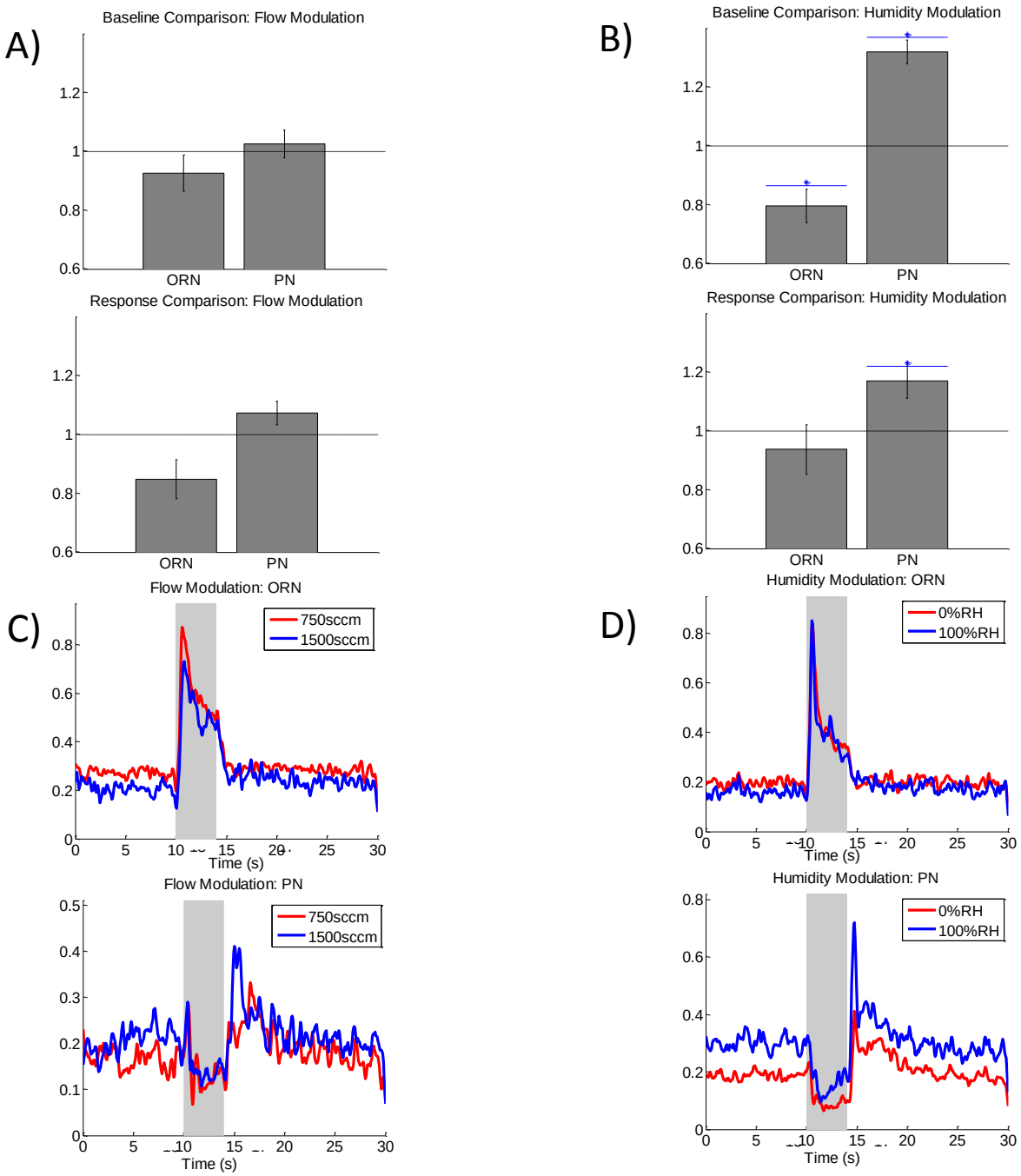

Figure 5.1: Changes in ORN baseline activity, not response magnitude, cause changes in PN response magnitude. A) Baseline and response magnitudes of the 1500sccm trials in the flow modulation experiments. Decreasing the ORN response magnitude did not change the PN baseline activity or response magnitude. B) Baseline and response magnitudes of the 100%RH trials in the flow modulation experiments. Decreases in the ORN baseline activity elicited changes in both baseline and response magnitude of the PNs. Dashed lines represent the normal test (750sccm or 0%RH, depending). Stars indicate significantly different from this normal test ($p < 0.05$). C&D) Mean traces for flow and humidity modulation experiments in ORNs and PNs. (Mean ± SEM)

I therefore conclude that the PNs play a compensatory role to changes ORN baseline activity to allow for a more robust response in the mushroom body as humidity changes (or, potentially, ORN baseline is altered by other outside factors). Changes in exclusively response magnitude, however, do not insight this compensatory mechanism, allowing the effects to reach all the way to the mushroom body. Because we have seen consistent response times and oscillatory behavior in the mushroom body, it is reasonable to assume that we have not changed the temporal dynamics of this system by introducing humidity to the air stream. Thus, the only changes elicited from adjusting the external factors (i.e., humidity and flow rate) are changes in the sum of neurons firing.

We have now shown that it is possible to alter the gain of the central olfactory circuit of the brain by changing the baseline receptor neuron firing activity through modulation of exogenous factors, i.e., humidity. It is possible that these downstream effects of the receptor neurons can be extended into other systems. For example, photoceptors in the eye, which hyperpolarize when stimulated with light, may elicit different responses in the visual processing circuit as a result of changes in their baseline activity [28]–[30]. Indeed, zebrafish have even exhibited changes in baseline movement behavior in different light stimuli [31]. It is possible that this is due to varying baseline activity in the photoreceptors.

5.2 Concerns and Future Work

One of the primary concerns with both ORN and PN experiments is the problem of undersampling. It is unfeasible to sample from all neurons, and therefore a subset must be used. In this work, in addition to a reasonable number of neurons being studied, the errors are low, and trends persist across the majority of neurons, so it can be assumed that the sampled neurons appropriately represent the overall population.

Clearly, the work done here has opened the door to many new questions regarding the effects of environmental factors on olfaction. In the future, it may be prudent to map the projection of ORNs in sensilla to see if there are any patterns regarding which projection areas are affected the most. This could potentially be done using a similar setup to the ORN recordings used currently, merely adding in a dye to the glass pipette, and using current to inject it into the ORNs. Additionally, even greater flow rates could be examined to see if there are further

interesting effects at higher flows. The trends shown here may persist or vanish, and new trends may appear.

References

[1] B. W. Ache and J. M. Young, “Olfaction: diverse species, conserved principles,” *Neuron*, vol. 48, no. 3, pp. 417–430, Nov. 2005.

[2] H. Baier and S. Korsching, “Olfactory glomeruli in the zebrafish form an invariant pattern and are identifiable across animals,” *J. Neurosci.*, vol. 14, no. 1, pp. 219–230, Jan. 1994.

[3] J. G. Hildebrand and G. M. Shepherd, “MECHANISMS OF OLFACTORY DISCRIMINATION:Converging Evidence for Common Principles Across Phyla,” *Annu. Rev. Neurosci.*, vol. 20, no. 1, pp. 595–631, 1997.

[4] R. I. Wilson and Z. F. Mainen, “Early Events in Olfactory Processing,” *Annu. Rev. Neurosci.*, vol. 29, no. 1, pp. 163–201, 2006.

[5] J. Boeckh, P. Distler, K. D. Ernst, M. Hösl, and D. Malun, “Olfactory Bulb and Antennal Lobe,” in *Chemosensory Information Processing*, D. Schild, Ed. Springer Berlin Heidelberg, 1990, pp. 201–227.

[6] N. J. Strausfeld, L. Hansen, Y. Li, R. S. Gomez, and K. Ito, “Evolution, Discovery, and Interpretations of Arthropod Mushroom Bodies,” *Learn. Mem.*, vol. 5, no. 1, pp. 11–37, May 1998.

[7] B. S. Hansson, S. A. Ochieng’, X. Grosmaitre, S. Anton, and P. G. N. Njagi, “Physiological responses and central nervous projections of antennal olfactory receptor neurons in the adult desert locust, Schistocerca gregaria (Orthoptera: Acrididae),” *J. Comp. Physiol. A*, vol. 179, no. 2, pp. 157–167, Aug. 1996.

[8] N. K. Tanaka, T. Awasaki, T. Shimada, and K. Ito, “Integration of Chemosensory Pathways in the Drosophila Second-Order Olfactory Centers,” *Curr. Biol.*, vol. 14, no. 6, pp. 449–457, Mar. 2004.

[9] M. de Bruyne, K. Foster, and J. R. Carlson, “Odor Coding in the Drosophila Antenna,” *Neuron*, vol. 30, no. 2, pp. 537–552, May 2001.

[10] D. Saha, K. Leong, C. Li, S. Peterson, G. Siegel, and B. Raman, “A spatiotemporal coding mechanism for background-invariant odor recognition,” *Nat. Neurosci.*, vol. 16, no. 12, pp. 1830–1839, Dec. 2013.

[11] B. Raman, J. Joseph, J. Tang, and M. Stopfer, "Temporally Diverse Firing Patterns in Olfactory Receptor Neurons Underlie Spatiotemporal Neural Codes for Odors," *J. Neurosci.*, vol. 30, no. 6, pp. 1994–2006, Feb. 2010.

[12] G. Laurent, M. Wehr, and H. Davidowitz, "Temporal representations of odors in an olfactory network," *J. Neurosci. Off. J. Soc. Neurosci.*, vol. 16, no. 12, pp. 3837–3847, Jun. 1996.

[13] J. S. de Belle and M. Heisenberg, "Associative odor learning in Drosophila abolished by chemical ablation of mushroom bodies," *Science*, vol. 263, no. 5147, pp. 692–695, Feb. 1994.

[14] S. Cassenaer and G. Laurent, "Conditional modulation of spike-timing-dependent plasticity for olfactory learning," *Nature*, vol. 482, no. 7383, pp. 47–52, Feb. 2012.

[15] I. Ito, M. Bazhenov, R. C. Ong, B. Raman, and M. Stopfer, "Frequency transitions in odor-evoked neural oscillations," *Neuron*, vol. 64, no. 5, pp. 692–706, Dec. 2009.

[16] J. Perez-Orive, O. Mazor, G. C. Turner, S. Cassenaer, R. I. Wilson, and G. Laurent, "Oscillations and Sparsening of Odor Representations in the Mushroom Body," *Science*, vol. 297, no. 5580, pp. 359–365, Jul. 2002.

[17] G. Laurent and M. Naraghi, "Odorant-induced oscillations in the mushroom bodies of the locust," *J. Neurosci.*, vol. 14, no. 5, pp. 2993–3004, May 1994.

[18] R. P. Akers and W. M. Getz, "A test of identified response classes among olfactory receptor neurons in the honey-bee worker," *Chem. Senses*, vol. 17, no. 2, pp. 191–209, Apr. 1992.

[19] M. Kuehn, H. Welsch, T. Zahnert, and T. Hummel, "Changes of pressure and humidity affect olfactory function," *Eur. Arch. Otorhinolaryngol.*, vol. 265, no. 3, pp. 299–302, Sep. 2007.

[20] C. Distante, N. Ancona, and P. Siciliano, "Support vector machines for olfactory signals recognition," *Sens. Actuators B Chem.*, vol. 88, no. 1, pp. 30–39, Jan. 2003.

[21] M. Begg and L. Hogben, "Chemoreceptivity of Drosophila melanogaster," *Proc. R. Soc. Lond. B Biol. Sci.*, vol. 133, no. 870, pp. 1–19, Jan. 1946.

[22] M. M. Mozell, P. F. Kent, and S. J. Murphy, “The effect of flow rate upon the magnitude of the olfactory response differs for different odorants,” *Chem. Senses*, vol. 16, no. 6, pp. 631–649, Dec. 1991.

[23] S. L. Youngentob, M. M. Mozell, P. R. Sheehe, and D. E. Hornung, “A quantitative analysis of sniffing strategies in rats performing odor detection tasks,” *Physiol. Behav.*, vol. 41, no. 1, pp. 59–69, 1987.

[24] D. Saha, K. Leong, N. Katta, and B. Raman, “Multi-unit Recording Methods to Characterize Neural Activity in the Locust (Schistocerca Americana) Olfactory Circuits,” *J. Vis. Exp.*, no. 71, Jan. 2013.

[25] D. Martinez, L. Arhidi, E. Demondion, J.-B. Masson, and P. Lucas, “Using Insect Electroantennogram Sensors on Autonomous Robots for Olfactory Searches,” *J. Vis. Exp.*, no. 90, Aug. 2014.

[26] R. K. Saini, M. M. Rai, A. Hassanali, J. Wawiye, and H. Odongo, “Semiochemicals from froth of egg pods attract ovipositing female Schistocerca gregaria,” *J. Insect Physiol.*, vol. 41, no. 8, pp. 711–716, Aug. 1995.

[27] R. Ignell, F. Couillaud, and S. Anton, “Juvenile-hormone-mediated plasticity of aggregation behaviour and olfactory processing in adult desert locusts,” *J. Exp. Biol.*, vol. 204, no. 2, pp. 249–259, Jan. 2001.

[28] M. del P. Gomez and E. Nasi, “Light Transduction in Invertebrate Hyperpolarizing Photoreceptors: Possible Involvement of a Go-Regulated Guanylate Cyclase,” *J. Neurosci.*, vol. 20, no. 14, pp. 5254–5263, Jul. 2000.

[29] A. L. F. Gorman, J. S. McReynolds, and S. N. Barnes, “Photoreceptors in Primitive Chordates: Fine Structure, Hyperpolarizing Receptor Potentials, and Evolution,” *Science*, vol. 172, no. 3987, pp. 1052–1054, Jun. 1971.

[30] S. Barnes, V. Merchant, and F. Mahmud, “Modulation of transmission gain by protons at the photoreceptor output synapse,” *Proc. Natl. Acad. Sci.*, vol. 90, no. 21, pp. 10081–10085, Nov. 1993.

[31] H. A. Burgess and M. Granato, “Modulation of locomotor activity in larval zebrafish during light adaptation,” *J. Exp. Biol.*, vol. 210, no. 14, pp. 2526–2539, Jul. 2007.

Vita

Matthew O'Neill

Degrees	M.S. Biomedical Engineering, Washington University in St. Louis, August 2015 B.S. Biomedical Engineering, University of Virginia, May 2013
Professional Societies	Biomedical Engineering Society